Quantization Analysis and Robust Design for Distributed Graph Filters

Saad, Leila Ben[1,2]; Beferull-Lozano, Baltasar[1,3]; Isufi, Elvin[4]
[1]Department of Information and Communication Technology (ICT) - University of Agder
[2]Department of Electrical engineering, Information Technology and Cybernetics - University of South-Eastern Norway
[3]SIGIPRO Department, SimulaMet, Simula Research Laboratory
[4]Faculty of Electrical Engineering, Mathematics and Computer Science, Delft University of Technology – The Netherlands

This is an Accepted Manuscript of an article published by IEEE in *IEEE Transactions on Signal Processing* on December 29, 2021, available online: https://doi.org/10.1109/TSP.2021.3139208

Saad, L. B., Beferull-Lozano, B. & Isufi, E. (2022). Quantization Analysis and Robust Design for Distributed Graph Filters. *IEEE Transactions on Signal Processing*, *70*, 643-658. https://doi.org/10.1109/TSP.2021.3139208

Quantization Analysis and Robust Design for Distributed Graph Filters

Leila Ben Saad, *Member, IEEE*, Baltasar Beferull-Lozano, *Senior Member, IEEE*, and Elvin Isufi, *Member, IEEE*

***Abstract*—Distributed graph filters have recently found applications in wireless sensor networks (WSNs) to solve distributed tasks such as reaching consensus, signal denoising, and reconstruction. However, when implemented over WSNs, the graph filters should deal with network limited energy constraints as well as processing and communication capabilities. Quantization plays a fundamental role to improve the latter but its effects on distributed graph filtering are little understood. WSNs are also prone to random link losses due to noise and interference. In this instance, the filter output is affected by both the quantization error and the topological randomness error, which, if it is not properly accounted in the filter design phase, may lead to an accumulated error through the filtering iterations and significantly degrade the performance. In this paper, we analyze how quantization affects distributed graph filtering over both time-invariant and time-varying graphs. We bring insights on the quantization effects for the two most common graph filters: the finite impulse response (FIR) and autoregressive moving average (ARMA) graph filter. Besides providing a comprehensive analysis, we devise theoretical performance guarantees on the filter performance when the quantization stepsize is fixed or changes dynamically over the filtering iterations. For FIR filters, we show that a dynamic quantization stepsize leads to more reduction of the quantization noise than in the fixed-stepsize quantization. For ARMA graph filters, we show that decreasing the quantization stepsize over the iterations reduces the quantization noise to zero at the steady-state. In addition, we propose robust filter design strategies that minimize the quantization noise for both time-invariant and time-varying networks. Numerical experiments on synthetic and two real data sets corroborate our findings and show the different trade-offs between quantization bits, filter order, and robustness to topological randomness.**

***Index Terms*—Distributed graph filtering, graph signal processing; graph filters; quantization; time-varying graphs.**

I. Introduction

GRAPH filters are enjoying an increasing popularity in graph signal processing (GSP) and graph convolutional neural networks [2], [3]. Their ability to be convolved with a graph signal renders graph filters versatile in a variety of applications ranging from recommender systems to spectral clustering [4-9]. Graph filters find also applications in wireless sensor networks (WSNs) [10-14]. Here, the signal represents the sensor measurements and the WSN serves as a platform to perform distributed operations as well as a proxy to represent signal similarities in adjacent sensor nodes. Graph filters are useful for distributed signal representation [15], reconstruction [16], [17], denoising [18], [19], consensus [20], [21] and network coding [22]. Motivated by these applications, this paper focuses on distributed graph filtering, considering also practical constraints within the context of WSNs.

Distributed graph filtering can be implemented with two types of recursions over the nodes: finite impulse response (FIR) and autoregressive moving average (ARMA) recursions. In FIR graph filters, neighboring nodes communicate the input signal for a finite number of iterations [18], [22-24]. In ARMA graph filters, neighboring nodes communicate both the input and former iterative output signal. Both implementations can be used interchangeably as basic filtering blocks and often lead to a different tradeoff between accuracy and robustness to topological perturbations. The works in [11], [25] show that ARMA filters can provide closed-form solutions to different inverse problems on graphs and are more robust than FIRs to deterministic topological changes (e.g. sensor movements), while [26] shows that higher order FIR graph filters suffer less from random topological changes (e.g. link losses).

For either implementation, in distributed filtering over WSNs, we should account for the understringent energy, processing and communication limitations of individual sensors. This motivates strongly the need of quantization to save energy and bandwidth of the sensor nodes performing cooperative actions in control, surveillance and weather monitoring tasks [10]. Thus, the quantization plays an important role prior to data communication in distributed graph filtering, where local node-to-node communication is required to reach a common objective in the network. Since traditional temporal filters and graph filters operate in different domains and are radically different [2], the quantization analysis in distributed graph filters is fundamentally different of that in the case of temporal filters and is more related to distributed signal processing. Quantization has been extensively studied in distributed systems in the context of communications and signal processing through consensus algorithms [27-34], which present many similarities with graph filtering from a distributed problem point-of-view. However, in consensus, the goal is to exchange quantized data to reach a consensus with respect to some global quantity, while with graph filters the goal is to exchange quantized data to perform any graph filtering task. The importance of quantization from the graph signal processing perspective has been recently recognized in [35-37]. In particular, [35] –the most related to our work– discusses the impact of fixed-stepsize quantization on FIR

This work was supported by the TOPPFORSK WISECART grant 250910/F20 and the IKTPLUSS INDURB grant 270730/O70 from the Research Council of Norway. Part of this work has been presented in [1].

L. Ben Saad is with the Department of Electrical Engineering, IT and Cybernetics, University of South-Eastern Norway, and WISENET center, University of Agder, Norway (e-mail: leila.b.saad@usn.no).

B. Beferull-Lozano is with the WISENET center, Department of Information and Communication Technology, University of Agder, Norway (e-mail: baltasar.beferull@uia.no). He is also with SIGIPRO Department, SimulaMet, Simula Research Laboratory (e-mail: baltasar@simula.no).

E. Isufi is with the Faculty of Electrical Engineering, Mathematics and Computer Science, Delft University of Technology, 2628 CD Delft, The Netherlands (e-mail: e.isufi-1@tudelft.nl).

graph filters. The work in [37] approximates the graph spectral dictionaries as polynomials of the graph Laplacian operator and learns polynomial dictionaries that are robust to signal quantization. Finally, [36] develops an adaptive quantization scheme for FIR graph filters that minimizes the quantization errors by bounding the exchanged messages and optimizing the bit allocation. While being relevant contributions on the quantization aspects of graph filtering, the limitation of these works is that they focus solely on FIR graph filters and fixed-stepsize quantization. Furthermore, they consider only time-invariant WSN topologies. This is a limitation in WSNs since sensor nodes are prone to local malfunctions or failure of communication links with a certain probability.

In this work, we analyze quantization effects of distributed graph filters (FIR and ARMA) on both time-invariant and time-varying topologies. Besides providing a broader analysis with an additional focus on time-varying graphs, we devise theoretical performance guarantees on the filter performance when the quantization stepsize is fixed or changes dynamically over the filtering iterations. We highlight also the benefits of such dynamic stepsize to reduce the quantization errors. Further, we consider dithered quantization [38], [39] to make the assumption of quantization noise uncorrelated with input signals over the different graph filter iterations hold; an assumption commonly made in other current works but unjustified. To reduce the communication cost, this work focuses on the quantization of the signals. To decrease further the energy consumption, the computational complexity of implementing the filter may be considered but this is beyond the current scope of the paper.

Our quantization effect analysis sheds light on different tradeoffs in distributed graph filtering over WSN: FIR versus ARMA graph filter; fixed-stepsize quantization versus dynamically decreasing quantization stepsizes; and quantization rate versus link loss probability. The overall research question we are interested in is *how quantization affects distributed graph filtering over both time-invariant and time-varying graphs.* The specific contributions of this paper in relation to this question are fourfold:

1) We investigate the quantization effects on distributed FIR graph filters. We analyze the impact of fixed and dynamic quantization stepsize on the filtering performance and analyze their tradeoffs. We show that a dynamic quantization stepsize allows to reduce more the quantization mean squared error (MSE) than in fixed-stepsize quantization. We devise also a robust filter design that minimizes the quantization noise.
2) We investigate the quantization effects on distributed ARMA graph filters. We analyze the impact of fixed and dynamic quantization stepsize on the filtering performance and analyze their tradeoffs. We develop an ad-hoc dynamic quantization stepsize strategy that reduces the quantization MSE to zero at the steady-state.
3) We perform a statistical analysis to quantify the quantization effects on FIR and ARMA graph filters over random time-varying networks, which has not been considered in previous work. We propose a novel filter design strategy that is robust to quantization and topological changes.
4) We characterize the different tradeoffs between the FIR and ARMA graph filters in terms of fixed-stepsize versus dynamically decreasing quantization stepsize and between the quantization rate and the link loss probability.

The rest of this paper is organized as follows. Section II provides the background material. Sections III and IV analyze the quantization effects on FIR and ARMA graph filters, respectively. Section V contains the quantization analysis for random time-varying graphs. Section VI presents the numerical results. The paper conclusions are provided in Section VII.

II. Background

Consider a graph $\mathcal{G} = (\mathcal{V}, \mathcal{E})$ with node set $\mathcal{V} = \{1, \ldots, N\}$ and $\mathcal{E} \subseteq \mathcal{V} \times \mathcal{V}$ the set of M edges, where $\mathcal{E}$ is composed of the tuples (j, i) if there is a link from node j to i. The set of all nodes connected to node i is denoted by $\mathcal{N}_i = \{j \in \mathcal{V} | (j, i) \in \mathcal{E}\}$. The graph can be represented by its adjacency matrix $\mathbf{A}$ whose (j, i)th entry is nonzero only if nodes j and i are connected. If the graph is undirected, it can also be represented by the graph Laplacian matrix $\mathbf{L}$, such as the discrete Laplacian $\mathbf{L}_{\text{d}} = \mathbf{D} - \mathbf{A}$ or normalized Laplacian $\mathbf{L}_{\text{n}} = \mathbf{D}^{-1/2}\mathbf{L}\mathbf{D}^{-1/2}$, with $\mathbf{D}$ is the diagonal degree matrix.

On the vertices of $\mathcal{G}$, a graph signal can be defined as a map from the vertex set (node set) to the set of real numbers, i.e., $x : \mathcal{V} \to \mathbb{R}$. We can denote the graph signal by a vector $\mathbf{x} = [x_1, \ldots, x_N]^{\mathsf{T}}$, whose ith entry x_i denotes the signal at node i. WSNs match the above terminology: the nodes represent the sensors; the edges the communication links; and the signal the sensor data. On the graph $\mathcal{G}$, we can also define the graph shift operator [2], [7], which is a local operation that replaces the signal value x_i at node i with a linear combination of values at the neighbors of node i. To keep the discussion general for both directed and undirected graphs, we will use as graph shift operator the matrix $\mathbf{S}$, which has plausible candidates $\mathbf{A}$, $\mathbf{L}$ or any of their normalized and translated forms [2]. We consider graphs for which $\mathbf{S}$ is real-valued and diagonalizable, and thus admits an eigenvalue decomposition $\mathbf{S} = \mathbf{U}\boldsymbol{\Lambda}\mathbf{U}^{-1}$ with eigenvector matrix $\mathbf{U} = [\mathbf{u}_1, \ldots, \mathbf{u}_N]$ and diagonal eigenvalue matrix $\boldsymbol{\Lambda} = \text{diag}(\lambda_1, \ldots, \lambda_N)$ [2], [23], where λ_1 up to λ_N denote the graph frequencies. In this work, we assume that the eigenvalues are real-valued and can be readily ordered from small to large. Complex eigenvalues can have ordering using the total variation measure, as proposed in [7]. This eigendecomposition holds for all undirected graphs based on the graph Laplacian and some directed graphs based on the adjacency matrix [7], [40], [41]. By considering the eigendecomposition of the graph shift operator, we can alternatively analyze the graph signal $\mathbf{x}$ by projecting it onto the shift operator eigenspace as $\hat{\mathbf{x}} = \mathbf{U}^{-1}\mathbf{x}$. This projection is referred to as the graph Fourier transform (GFT) because the ith element $\hat{x}_i$ denotes how much eigenvector $\mathbf{u}_i$ represents the variation of $\mathbf{x}$ over $\mathcal{G}$ and because the variation of the different eigenvectors can be ordered. The inverse GFT is $\mathbf{x} = \mathbf{U}\hat{\mathbf{x}}$. We shall assume that the shift operator has an upper bounded spectral norm, i.e., $\|\mathbf{S}\|_2 \leq \rho < \infty$ where ρ denotes the spectral radius of $\mathbf{S}$. Since any matrix $\mathbf{S}$ with entries S_{ij} has bounded spectral norm $\|\mathbf{S}\|_2 < \infty$, in practice, this also

means the graphs of interest have finite dimension and edge weights, as shown in [42], [43]. An upper bounded spectral norm of the shift operator $\mathbf{S}$ implies also that the maximum eigenvalue of $\mathbf{S}$ is upper bounded. For example, for Laplacian matrices $\mathbf{L}$ belonging to a set $\mathcal{L}$, the minimum eigenvalue is bounded below by $\lambda_{\min}$ and the maximum eigenvalue is bounded above by $\lambda_{\max}$ i.e., $||\mathbf{L}||_2 \leq \rho = \max\{|\lambda_{\min}|, |\lambda_{\max}|\}$. More specifically, for discrete Laplacian $\mathbf{L} = \mathbf{L}_{\text{d}}$, we can take $\lambda_{\min} = 0$ and $\lambda_{\max}$ related to the maximum eigenvalue of any of the graphs, while for the normalized Laplacian $\mathbf{L} = \mathbf{L}_{\text{n}}$, we can take $\lambda_{\min} = 0$ and $\lambda_{\max} = 2$.

A. Graph filter

A one-hop filtering operation on a graph combines locally the signal from node i and the signals $\{x_j\}$ from all neighbors $j \in \mathcal{N}_i$ of node i to generate the output:

$$y_i = \sum_{j \in \mathcal{N}_i \cup i} \phi_{ij} x_j \tag{1}$$

for some scalar coefficients ϕ_{ij}. By stacking all nodes' outputs in one vector $\mathbf{y} = [y_1, \ldots, y_N]^{\mathsf{T}}$, and performing several consecutive one-hop filtering operations as in (1) with exchanges of information among neighbors, we obtain $\mathbf{y} = \mathbf{H}(\mathbf{S})\mathbf{x}$, where the matrix $\mathbf{H}(\mathbf{S}) : \mathbb{R}^N \to \mathbb{R}^N$ denotes the graph filter. The graph filter can be expressed as a function of the shift operator $\mathbf{S}$ in different ways. Two widely used approaches[1] are the FIR graph filter [22], [23] and the ARMA graph filter [11], [41].

FIR. An FIR graph filter is a polynomial of order K in the shift operator $\mathbf{S}$ with output:

$$\mathbf{y} = \mathbf{H}(\mathbf{S})\mathbf{x} = \sum_{k=0}^{K} \phi_k \mathbf{S}^k \mathbf{x} \tag{2}$$

and scalar coefficients $\phi_0, \ldots, \phi_K$. The filtering behavior of $\mathbf{H}(\mathbf{S})$ can be viewed by means of the GFT:

$$h(\lambda) = \sum_{k=0}^{K} \phi_k \lambda^k \quad \text{for} \quad \lambda \in [\lambda_{\min}, \lambda_{\max}] \tag{3}$$

which is a polynomial in the generic graph frequency λ. This spectral representation allows to define a filtering operator by specifying the analytic function $h(\lambda) : [\lambda_{\min}, \lambda_{\max}] \to \mathbb{R}$; hence, by approximating the latter with the polynomial in (3), we can implement it distributively over the nodes through the recursion (2) [18]. The distributed implementation is feasible because the shifted signal $\mathbf{x}^{(1)} = \mathbf{S}\mathbf{x}$ can be obtained through local exchanges between neighboring nodes in one communication iterate [cf. (1)]. The kth shifted signal can be obtained recursively as $\mathbf{x}^{(k)} = \mathbf{S}\mathbf{x}^{(k-1)}$, where nodes communicate to their neighbors the shifted signal $\mathbf{x}^{(k-1)}$ obtained in the $(k-1)$th communication iterate. The output $\mathbf{y}$ of the FIR graph filter is obtained after K iterations of exchanges between neighbors, implying that in total, each node i exchanges $K\text{deg}(i)$ messages with its neighbors. This yields a communication complexity of order $\mathcal{O}(MK)$ [11].

[1]Recent works consider also more general approaches such as the node-variant [22] and the edge-variant graph filter [24]. To keep the exposition simple, we will discuss quantization of the two baseline approaches and leave the extension to the other methods for future research.

ARMA. The ARMA graph filter extends (3) to a rational spectral response [11]:

$$h(\lambda) = \frac{\sum_{q=0}^{Q} b_q \lambda^q}{1 + \sum_{p=1}^{P} a_p \lambda^p} = \sum_{k=1}^{K} \left(\frac{\varphi_k}{1 - \lambda \psi_k} \right) + \sum_{l=1}^{L} \phi_l \lambda^l \quad \text{for} \quad \lambda \in [\lambda_{\min}, \lambda_{\max}] \tag{4}$$

which allows for more flexibility when designing the filter coefficients $a_1, \ldots, a_P$ and $b_0, \ldots, b_Q$ (or the respective roots $\varphi_1, \ldots, \varphi_K$, poles $\psi_1, \ldots, \psi_K$, and direct term $\phi_1, \ldots, \phi_L$ coefficients) [41]. Without loss of generality, we consider $L = 0$ and refer to the filter in right-side of (4) as an ARMA$_K$ graph filter [11].

We can implement the ARMA$_K$ graph filter through the iterative recursion:

$$\begin{aligned} \mathbf{w}_t^{(k)} &= \psi_k \mathbf{S} \mathbf{w}_{t-1}^{(k)} + \varphi_k \mathbf{x} \\ \mathbf{y}_t &= \sum_{k=1}^{K} \mathbf{w}_t^{(k)} \qquad \text{for } t \geq 1 \end{aligned} \tag{5}$$

where $\mathbf{y}_t$ is the ARMA$_K$ output at iteration t and $\mathbf{w}_t^{(k)}$ is the output of the kth branch at iteration t with arbitrary initialization $\mathbf{w}^{(0)}$. Recursion (5) builds the overall output $\mathbf{y}_t$ at iteration t as the sum of all K parallel branches outputs $\mathbf{w}_t^{(k)}$ and converges ($t \to \infty$) to a steady-state only if the roots satisfy $|\psi_k| \leq \rho$ for all $k = 1, \ldots, K$, where ρ is the spectral radius of $\mathbf{S}$ [11].

The output of each branch $\mathbf{w}_t^{(k)}$ can be implemented distributively in a similar way as the FIR filters. The difference is that neighboring nodes exchange now the former output $\mathbf{w}_{t-1}^{(k)}$. Node i combines the shifted outputs $w_{jt}^{(k)}$ from all neighbors $j \in \mathcal{N}_i$ with its input signal x_i with coefficients (as given in (5)) to obtain the output $w_{it}^{(k)}$. Finally, node i combines locally all branches' outputs $w_{ti}^{(1)}, \ldots, w_{ti}^{(K)}$ to obtain the overall ARMA$_K$ output y_{it} at iteration t. This procedure accounts for K communications between neighbors at each iteration t; hence, the overall communication cost of the ARMA$_K$ filter for $t = t_{\text{max}}$ iterations is of order $\mathcal{O}(MKt_{\text{max}})$ [11].

Expressions (2) and (5) represent two fundamental algorithms to implement distributed GSP operations over WSNs. Our goal is to analyze the effects of dithered quantization to the filter outputs and account for it in the filter design phase. We shall analyze first quantization effects for static topologies in Sections III and IV and later for random time-varying topologies in Section V. Before proceeding with this analysis for the FIR graph filters, let us briefly introduce the conceptual terminology of dithered quantization.

B. Dithered quantization

Quantization consists of encoding the data prior to its transmission with a certain number of bits, reducing the amount of information to be transmitted as compared to the initial data [44]. During the quantization, the information is compressed in a lossy manner due to a round-off error generated in a finite-precision machine.

Uniform quantizers map each input signal value to the nearest value of a finite set of quantization levels, where the quantization stepsize between two adjacent levels is constant

[45]. The mapping of a uniform quantizer $Q : \mathbb{R} \to [-r, r]$ is expressed as $Q(x) \triangleq \Delta([\frac{x}{\Delta}] + \frac{1}{2})$ for $|x| < r$, where B is the number of levels, $b = \log_2(B)$ is the number of bits, r is the dynamic range, and $\Delta = \frac{2\,r}{B}$ is the stepsize. We denote the quantized version of signal $\mathbf{x}$ as $\tilde{\mathbf{x}} = Q(\mathbf{x})$, and it is given by:

$$\tilde{\mathbf{x}} = \mathbf{x} + \mathbf{n}_{\mathrm{q}} \tag{6}$$

where $\mathbf{n}_{\mathrm{q}}$ is the quantization noise. Although the quantization noise is deterministic, for a sufficiently small quantization stepsize Δ (high rate conditions), it can be well modeled as a uniformly random variable with zero-mean and variance $\Delta^2/12$, that is independent from the input [39], [46].

In order to give the quantization noise certain desirable properties that ensure the zero-mean uniform random variable assumption with variance $\Delta^2/12$ and independence from the input, we consider in this work dithering quantization [38], [39], [46]. Dithering consists of adding a random additive signal $\mathbf{n}_{\mathrm{d}}$, called dither, to the input signal $\mathbf{x}$ prior to quantization. Dithering is widely used in distributed signal processing [28], [31], [34], [47], which consists of iterative algorithms akin to distributed graph filtering. In subtractive dithered quantization, the dither signal is generated by a pseudo-random generator at the transmitter node and it is subtracted at the receiving node after transmission. The receiver node uses the same pseudo-random generator, which needs to be agreed prior to starting the communication. Let us denote $\mathbf{x}_{\mathrm{d}} = \mathbf{x} + \mathbf{n}_{\mathrm{d}}$ the dithered signal of $\mathbf{x}$. By applying quantization to the dithered signal $\mathbf{x}_{\mathrm{d}}$, the transmitted signal becomes:

$$\tilde{\mathbf{x}}_{\mathrm{d}} = Q(\mathbf{x}_{\mathrm{d}}) = Q(\mathbf{x} + \mathbf{n}_{\mathrm{d}}) = \mathbf{x} + \mathbf{n}_{\mathrm{d}} + \mathbf{n}_{\mathrm{q}} = \tilde{\mathbf{x}} + \mathbf{n}_{\mathrm{d}} \tag{7}$$

where signal $\tilde{\mathbf{x}}$ can be recovered by the receiver node by subtracting the dither $\mathbf{n}_{\mathrm{d}}$ from the received signal $\tilde{\mathbf{x}}_{\mathrm{d}}$.

The dither signal $\mathbf{n}_{\mathrm{d}}$ follows an i.i.d. uniform distribution with first and second order moments:

$$\mathbb{E}[\mathbf{n}_{\mathrm{d}}] = \mathbf{0} \text{ and } \boldsymbol{\Sigma}_{\mathrm{d}} = \sigma_{\mathrm{d}}^2 \mathbf{I} = \frac{\Delta^2}{12}\mathbf{I}. \tag{8}$$

The quantization noise $\mathbf{n}_{\mathrm{q}}$ also follows a uniform distribution with statistical properties:

$$\mathbb{E}[\mathbf{n}_{\mathrm{q}}] = \mathbf{0} \text{ and } \boldsymbol{\Sigma}_{\mathrm{q}} = \sigma_{\mathrm{q}}^2 \mathbf{I} = \frac{\Delta^2}{12}\mathbf{I} \tag{9}$$

and with realisations independent of the input.

Note that for this model to hold, we are considering that the entries of $\mathbf{x}+\mathbf{n}_{\mathrm{d}}$ should be scaled to reside with high probability in the dynamic quantization range (not overfloading) and the probability of overfloading of the quantizer is sufficiently small i.e., $\Pr(|(\mathbf{x} + \mathbf{n}_{\mathrm{d}})_i)| > r_i) \approx 0$ for each $i \in 1 \cdots N$, by fixing $r_i^2 = \vartheta^2 \mathbb{E}\{(\mathbf{x} + \mathbf{n}_{\mathrm{d}})_i^2\}$, with ϑ is some multiple number, as adopted in [48], [49].

Two possible cases can be adopted when performing quantization with substractive dithering, namely, a constant quantization stepsize for all iterations or a dynamically decreasing quantization stepsize over the iterations, which offers a benefit as compared to a fixed quantization stepsize. Decreasing the quantization stepsize implies transmitting more bits over the iterations, but it can reduce the quantization noise or even make it converge to zero. In the sequel, we will analyze both cases.

III. FIR QUANTIZATION ANALYSIS

This section analyzes the quantization effects in FIR graph filters. We first discuss the fixed quantization stepsize and then the dynamically decreasing stepsize. Next, we formulate a filter design problem that is robust to quantization noise.

A. Fixed quantization stepsize

Consider the kth shifted signal $\mathbf{x}^{(k)} = \mathbf{S}^k\mathbf{x}$ exchanged with the neighbors. The quantized form of the latter is $\tilde{\mathbf{x}}^{(k)} = Q(\mathbf{x}^{(k)}) = \mathbf{x}^{(k)} + \mathbf{n}_{\mathrm{q}}^{(k)}$. At the filter initialization, we have $\mathbf{x}^{(0)} = \mathbf{x}$, which quantized form is $\tilde{\mathbf{x}}^{(0)} = \mathbf{x}^{(0)} + \mathbf{n}_{\mathrm{q}}^{(0)}$. This quantized signal is exchanged with neighbors leading to the quantized shifted signal $\mathbf{x}^{(1)} = \mathbf{S}\tilde{\mathbf{x}}^{(0)} = \mathbf{S}(\mathbf{x}^{(0)} + \mathbf{n}_{\mathrm{q}}^{(0)})$. Signal $\mathbf{x}^{(1)}$ is further quantized into $\tilde{\mathbf{x}}^{(1)}$ and subsequently transmitted to the neighboring nodes. The process is repeated K times. Based on the derivation in Appendix VIII-A, the FIR filter output [cf. (2)] with quantization becomes:

$$\mathbf{y}^{\mathrm{q}} = \sum_{k=0}^{K} \phi_k \mathbf{S}^k \mathbf{x} + \sum_{k=1}^{K} \phi_k \sum_{\kappa=0}^{k-1} \mathbf{S}^{k-\kappa} \mathbf{n}_{\mathrm{q}}^{(\kappa)} \tag{10}$$

where the second term on the right-hand side of (10) accounts for the accumulated quantization error on the output:

$$\boldsymbol{\epsilon} = \mathbf{y}^{\mathrm{q}} - \mathbf{y} = \sum_{k=1}^{K} \phi_k \sum_{\kappa=0}^{k-1} \mathbf{S}^{k-\kappa} \mathbf{n}_{\mathrm{q}}^{(\kappa)}. \tag{11}$$

We analyze next this quantization error in the spectral domain to ease the filter design. The following proposition provides a closed-form expression of the quantization MSE.

Proposition 1. *Consider the FIR graph filter of order K in (2) with coefficients $\phi_0, \ldots, \phi_K$ and quantization error $\boldsymbol{\epsilon}$ in (11) under fixed quantization stepsize. Consider also the graph Fourier transform $\hat{\boldsymbol{\epsilon}} = \mathbf{U}^{-1}\boldsymbol{\epsilon}$ of the error with respect to the shift operator $\mathbf{S} = \mathbf{U}\boldsymbol{\Lambda}\mathbf{U}^{-1}$. The average quantization MSE per node $\hat{\zeta}_q = \mathbb{E}\left[\frac{1}{N} tr(\hat{\boldsymbol{\epsilon}}\hat{\boldsymbol{\epsilon}}^H)\right]$ is:*

$$\hat{\zeta}_q = \frac{\sigma_{\mathrm{q}}^2}{N} \sum_{k=1}^{K} \phi_k^2 \sum_{\kappa=0}^{k-1} \|\boldsymbol{\Lambda}^{k-\kappa}\|_F^2. \tag{12}$$

where $\|\cdot\|_F$ denotes the Frobenius norm and σ_{q} is the uniform quantizer standard deviation.

Proof: See Appendix VIII-B. □

Proposition 1 characterizes the impact of the graph frequencies $\boldsymbol{\Lambda}$ on the quantization in FIR graph filters. A shift operator with large eigenvalues amplifies the quantization MSE. This is because the high frequency terms contribute more to the quantization noise. In other words, shift operators with small spectral radius bounds are preferred (e.g., normalized Laplacian or adjacency matrix). The filter coefficients $\phi_1, \ldots, \phi_K$ play also a role in the quantization error. As such, we can leverage expression (12) to reduce the quantization MSE in the design phase, as suggested by [35]. While expression (12) is useful if the eigendecomposition of the shift operator is computationally feasible, we can easily bound it by using the maximum eigenvalue. The latter can be estimated with a lighter computational cost via power methods [50].

Corollary 1.1. *Given the hypothesis of **Proposition 1**, the quantization MSE on the filter output $\hat{\zeta}_q$ is always lower*

and upper-bounded. If the shift operator $\mathbf{S}$ *has a maximum eigenvalue* $\lambda_{max} \neq 1$*, we can find closed form for these lower and upper bounds*[2]*:*

$$\frac{\sigma_q^2}{N}\sum_{k=1}^{K}\phi_k^2\ \eta_k \leq \hat{\zeta}_q \leq \sigma_q^2\sum_{k=1}^{K}\phi_k^2\ \eta_k \tag{13}$$

where $\eta_k = (1-\lambda_{max}^2)^{-1}(\lambda_{max}^2 - (\lambda_{\max}^2)^{k+1})$.

Proof: See Appendix VIII-C. □

The bounds in (13) suggest that by working with a fixed quantization stepsize, the MSE has always a *Cramer-Rao lower-bound equivalence* [51], which cannot be overcome even by tuning the FIR coefficients in the design phase. In other words, even with a robust design strategy as the one in [35], we have an unavoidable error due to quantization that will affect the filter frequency response. To tackle this issue, next, we propose an approach based on dynamically decreasing the quantization stepsize, which has the benefit to reduce the MSE.

B. Dynamically decreasing quantization stepsize

Consider the quantization stepsize Δ_k, which is defined as the ratio of the quantization range r_k at iterate k over the number of quantization intervals, is given by $\Delta_k = r_k/2^{b_k}$, where b_k is the number of bits transmitted at iterate k. Let us assume that with high probability, the entries of the input signal are such that $x_{\text{low}} \leq (\mathbf{x}+\mathbf{n}_{\text{d}})_i \leq x_{\text{upp}}$ for $i \in 1\cdots N$. The quantization stepsize can then be expressed as $\Delta_k = (x_{\text{upp}} - x_{\text{low}})/2^{b_k}$. We assume here a fixed quantization range over the iterations and a fix length codeword. By decreasing Δ_k at each iterate k, more bits $b_k = \log_2((x_{\text{upp}} - x_{\text{low}})/\Delta_k)$ will be transmitted for the higher filter iterates ($k \to K$). The main result is given by the following proposition.

Proposition 2. *Consider the FIR graph filter with shift operator* $\mathbf{S}$ *such that* $0 \leq \lambda_{max} \leq 1$*. Consider also that the input signal is quantized with a uniform quantizer, where the quantization stepsize* $\Delta_k = (\lambda_{max})^k\Delta_0$ *is decreasing over the iterates* k*. Then, the quantization MSE* $\hat{\zeta}_q$ *of the FIR graph filter is upper bounded by*[3]*:*

$$\hat{\zeta}_q \leq \frac{\Delta_0^2}{12}\mathbf{r}^\top\boldsymbol{\phi}_1 \tag{14}$$

where $\mathbf{r} = [1,2,\cdots,K]^\top$ *and* $\boldsymbol{\phi}_1 = [\phi_1^2,\phi_2^2,\cdots,\phi_K^2]^\top$ *is the vector containing squared FIR coefficients for* $k = 1,\cdots,K$*.*

Proof: See Appendix VIII-D. □

As opposed to Proposition 1, expression (14) shows that we can clearly minimize the quantization MSE through $\boldsymbol{\phi}_1$. Indeed, during the filter design phase, if we impose for the filter coefficients the condition that $\mathbf{r}^\top\boldsymbol{\phi}_1 \approx 0$, we can reduce significantly the quantization MSE.

There exists clearly a trade-off between the quantization MSE and the number of transmitted bits. For a small filter order K, a decreasing stepsize can be adopted, providing lower quantization MSE at the cost of more bits transmitted, as compared to the use of a fixed quantization stepsize, while for large filter orders K, a fixed stepsize can be adopted at the cost of higher quantization MSE. To reduce the quantization MSE at the beginning and limit the communication cost in the end, an alternative could be using decreasing stepsizes at the beginning and then switching to start using the initial given stepsize Δ_0 if the number of bits transmitted after some iterates exceeds a certain threshold.

[2]If the maximum eigenvalue $\lambda_{\max}$ is exactly 1, we can still add a small perturbation to it to make our assumption hold.

[3]The condition $0 \leq \lambda_{\max} \leq 1$ can be easily met in practice by appropriately selecting the shift operator (e.g, translated forms of Laplacian).

C. Filter design

Given a desired frequency response $h^*(\lambda)$, we propose to design an FIR graph filter by solving the following convex optimization problem:

$$\begin{aligned}
\underset{\phi_0,\ldots,\phi_K}{\text{minimize}} \quad & \int_\lambda \left|\sum_{k=0}^{K}\phi_k\lambda^k - h^*(\lambda)\right|^2 d\lambda \\
\text{subject to} \quad & \frac{1}{12}\sum_{k=1}^{K}\phi_k^2\sum_{\kappa=0}^{k-1}\Delta_\kappa^2(\lambda_{\max}^2)^{k-\kappa} \leq \epsilon \\
& \mathbf{r}^\top\boldsymbol{\phi}_1 \leq \gamma \\
& \delta_{\min} \leq \Delta_k \leq \delta_{\max},\quad k \in [0,1,2,\ldots,K]
\end{aligned} \tag{15}$$

For a finite small constant ϵ, the first constraint upper bound the quantization MSE in the cases of both fixed and decreasing quantization stepsizes [cf. (52)]. The second constraint aims to further reduce the quantization MSE where decreasing quantization stepsize is used through $\boldsymbol{\phi}_1$. For an infinite value of γ, (15) leads to a similar optimization problem in [35] for the case of fixed quantization stepsize, while for the case of decreasing quantization stepsize, a finite small γ can be used. In the last constraint, $\delta_{\min}$ and $\delta_{\max}$ represents, respectively, the minimum and maximum quantization stepsize at each iterate. The minimum quantization stepsize $\delta_{\min}$ implies also a restriction on the maximum number of bits χ that can be used at each iterate.

Let b be the average number of bits transmitted over the iterates. By quantizing the initial data of b_0 bits with b (i.e., $b < b_0$), the communication cost of FIR graph filter in term of number of bits exchanged reduces to $\mathcal{O}(MKb)$. The latter can be obtained similarily to Section II-A or in [11], [24], [26].

IV. ARMA QUANTIZATION ANALYSIS

This section analyzes the quantization effects on distributed ARMA graph filters. Since ARMA filters reach the designed frequency response at steady-state, the signal quantization will have also an effect on the filter convergence. We show in this section that the overall quantized MSE converges to zero if a dynamically decreasing quantization stepsize is considered, while this is not the case for the fixed stepsize-size quantizer.

A. Fixed quantization stepsize

Consider the parallel ARMA_K graph filter in (5) and let us indicate by $\mathbf{w}_t^{\text{q}(k)} = Q(\mathbf{w}_t^{(k)}) = \mathbf{w}_t^{(k)} + \mathbf{n}_t^{\text{q}(k)}$ the quantized signal of branch k at iteration t, i.e., $\mathbf{w}_t^{(k)}$. Here, $\mathbf{n}_t^{\text{q}(k)}$ denotes the respective quantization noise. Let also $\mathbf{w}_t = [{\mathbf{w}_t^{(1)}}^\top, {\mathbf{w}_t^{(2)}}^\top, \cdots, {\mathbf{w}_t^{(K)}}^\top]^\top$ be the $NK \times 1$ stacked vector containing all branches outputs and $\mathbf{n}_t^{\text{q}} = [{\mathbf{n}_t^{\text{q}(1)}}^\top, {\mathbf{n}_t^{\text{q}(2)}}^\top, \cdots, {\mathbf{n}_t^{\text{q}(K)}}^\top]^\top$ the $NK \times 1$ stacked vector of quantization noise. Then, we can write the ARMA output $\mathbf{y}_t$ due to quantization with the following compact notation:

$$\begin{aligned}\mathbf{w}_t^{\mathrm{q}} &= (\boldsymbol{\Psi}\otimes\mathbf{S})(\mathbf{w}_{t-1}^{\mathrm{q}}+\mathbf{n}_{t-1}^{\mathrm{q}})+\boldsymbol{\varphi}\otimes\mathbf{x}\\ \mathbf{y}_t^{\mathrm{q}} &= (\mathbf{1}^\top\otimes\mathbf{I}_N)\mathbf{w}_t^{\mathrm{q}}\end{aligned}\quad \text{for } t\geq 1 \tag{16}$$

where $\otimes$ indicates the Kronecker product, $\boldsymbol{\Psi} = \mathrm{diag}(\psi_1,\psi_2,\cdots,\psi_K)$ is the $K\times K$ diagonal matrix containing the former-output coefficients in the main diagonal and $\boldsymbol{\varphi}=[\varphi_1,\varphi_2,\cdots,\varphi_k]^\top$ is the $K\times 1$ coeffcient vector associated to the input. By unfolding $\mathbf{w}_t^{\mathrm{q}}$ in (16) to all its terms, we have:

$$\mathbf{w}_t^{\mathrm{q}} = (\boldsymbol{\Psi}\otimes\mathbf{S})^t\mathbf{w}_0+\sum_{\tau=0}^{t-1}(\boldsymbol{\Psi}\otimes\mathbf{S})^\tau(\boldsymbol{\varphi}\otimes\mathbf{x})+\sum_{\tau=0}^{t-1}(\boldsymbol{\Psi}\otimes\mathbf{S})^{t-\tau}\mathbf{n}_\tau^{\mathrm{q}} \tag{17}$$

where the first two terms on the right-hand side account for the ARMA output up to iteration t, while the third term $\boldsymbol{\epsilon}_t^{\mathrm{q}} = \sum_{\tau=0}^{t-1}(\boldsymbol{\Psi}\otimes\mathbf{S})^{t-\tau}\mathbf{n}_\tau^{\mathrm{q}}$ accounts for the accumulated quantization noise.

To analyze the MSE for the ARMA filter, let us first denote by $\mathbf{w}^*=\lim_{t\to\infty}\mathbf{w}_t^{\mathrm{q}}$ and by $\mathbf{y}^*=\lim_{t\to\infty}\mathbf{y}_t^{\mathrm{q}}$ the steady-state values of $\mathbf{w}_t^{\mathrm{q}}$ and $\mathbf{y}_t^{\mathrm{q}}$ in (16), respectively. Let us also define the error:

$$\boldsymbol{\epsilon}_t^* = (\boldsymbol{\Psi}\otimes\mathbf{S})^t\mathbf{w}_0+\sum_{\tau=0}^{t-1}(\boldsymbol{\Psi}\otimes\mathbf{S})^\tau(\boldsymbol{\varphi}\otimes\mathbf{x})-\mathbf{w}^* \tag{18}$$

which indicates how close the output of all branches $\mathbf{w}_t$ (without quantization) at iteration t are w.r.t. the steady-state value $\mathbf{w}^*$. We consider also the error $\boldsymbol{\epsilon}_{yt}=\mathbf{y}_t^{\mathrm{q}}-\mathbf{y}^*$ between the quantized ARMA output $\mathbf{y}_t^{\mathrm{q}}$ in (16) and the steady-state output $\mathbf{y}^*$, which can be written as follows:

$$\boldsymbol{\epsilon}_{yt} = (\mathbf{1}^\top\otimes\mathbf{I}_N)\boldsymbol{\epsilon}_t^*+(\mathbf{1}^\top\otimes\mathbf{I}_N)\boldsymbol{\epsilon}_t^{\mathrm{q}} = \boldsymbol{\epsilon}_{yt}^*+\boldsymbol{\epsilon}_{yt}^{\mathrm{q}} \tag{19}$$

where $\boldsymbol{\epsilon}_{yt}^* = (\mathbf{1}^\top\otimes\mathbf{I}_N)\boldsymbol{\epsilon}_t^*$ indicates how close the *unquantized* ARMA filter output $\mathbf{y}_t$ at iteration t is w.r.t. its steady-state $\mathbf{y}^*$ and $\boldsymbol{\epsilon}_{yt}^{\mathrm{q}} = (\mathbf{1}^\top\otimes\mathbf{I}_N)\boldsymbol{\epsilon}_t^{\mathrm{q}}$ accounts for the propagation of the quantization noise over the iterations. Then by simple algebra, the average MSE deviation per node of the error $\boldsymbol{\epsilon}_{yt}$ in (19) can be similarly split as:

$$\zeta_{yt} = \frac{1}{N}\mathbb{E}[\mathrm{tr}(\boldsymbol{\epsilon}_{yt}\boldsymbol{\epsilon}_{yt}^{\mathrm{H}})] = \zeta_{yt}^*+\zeta_{yt}^{\mathrm{q}} \tag{20a}$$

with:

$$\zeta_{yt}^* = \frac{1}{N}\mathbb{E}[\mathrm{tr}((\mathbf{1}^\top\otimes\mathbf{I}_N)\boldsymbol{\epsilon}_t^*\boldsymbol{\epsilon}_t^{*\mathrm{H}}(\mathbf{1}^\top\otimes\mathbf{I}_N)^{\mathrm{H}})] \tag{20b}$$

$$\zeta_{yt}^{\mathrm{q}} = \frac{1}{N}\mathbb{E}[\mathrm{tr}((\mathbf{1}^\top\otimes\mathbf{I}_N)\boldsymbol{\epsilon}_t^{\mathrm{q}}\boldsymbol{\epsilon}_t^{\mathrm{q}\mathrm{H}}(\mathbf{1}^\top\otimes\mathbf{I}_N)^{\mathrm{H}})] \tag{20c}$$

where we have used the linearity of the expectation w.r.t the trace and the independence of $\mathbf{x}$, $\mathbf{w}_0$ and $\mathbf{n}_\tau^{\mathrm{q}}$. ζ_{yt}^* is the MSE for the case of unquantized filter output from the steady-state output and ζ_{yt}^{q} is the quantization MSE at iteration t. The following proposition provides an upper bound on the quantization MSE.

Proposition 3. *Consider the ARMA$_K$ graph filter of order K in* (16) *with coefficients $\boldsymbol{\Psi}$ and $\boldsymbol{\varphi}$, and quantization error $\boldsymbol{\epsilon}_{yt}^q$. Let $\psi_{max}=max(|\psi_1|,|\psi_2|,\cdots,|\psi_K|)$ be the ARMA$_K$ coefficient with largest magnitude and let all ARMA$_K$ branches be stable i.e., $\psi_{max}\lambda_{max}<1$ for all $k=1\cdots K$. Consider also that the signal is quantized with a uniform quantizer with a fixed quantization stepsize Δ. The quantization MSE ζ_{yt}^q of the filter at iteration t is upper bounded by:*

$$\zeta_{yt}^q \leq K\sigma_q^2\frac{(\psi_{max}\lambda_{max})^2-\left((\psi_{max}\lambda_{max})^2\right)^{t+1}}{1-(\psi_{max}\lambda_{max})^2}. \tag{21}$$

Further, the steady-state ($t\to\infty$) quantization MSE is:

$$\zeta_{yt\to\infty}^q \leq K\sigma_q^2\frac{(\psi_{max}\lambda_{max})^2}{1-(\psi_{max}\lambda_{max})^2}. \tag{22}$$

Proof: See Appendix VIII-E. □

Proposition 3 shows that the quantization MSE ζ_{yt}^{q} of ARMA graph filters is upper bounded by a term that depends on the shift operator maximum eigenvalue. At steady-state $t\to\infty$, the overall ARMA MSE in (20a) is governed by the quantization MSE ζ_{yt}^{q} since the deviation ζ_{yt} from the steady-state vanishes $\zeta_{yt\to\infty}^*\to 0$ for convergent stable filters. Therefore, we conclude that a fixed quantization stepsize heavily affects the ARMA filter behavior, which even at the steady-state, although not divergent, might lead to a completely different filtering behavior.

The filtering behavior of the ARMA recursion will not be considerably affected by the quantization noise in the early regime (i.e., small value of t) as long as:

$$\zeta_{yt}^* \gg \zeta_{yt}^{\mathrm{q}}. \tag{23}$$

However, for larger t, this inequality will be violated and the overall ARMA MSE will by dominated by the quantization MSE ζ_{yt}^{q}. While we might control (3) in the design phase of FIR graph filters, we should consider the challenges encountered when designing convergent distributed ARMA filters [11], i.e., the difficulty to guarantee an accuracy-quantization robustness tradeoff. Rephrasing a non-convex design problem akin to (15) is possible, but because of non-convexity that may lead to suboptimal design solutions, in this work, we tackle this challenge by considering a decreasing quantization stepsize with t.

B. Dynamically decreasing quantization stepsize

Consider now a dynamic quantization stepsize Δ_t that decreases with t in a form that the quantization MSE ζ_{yt}^{q} decreases with t at least with the rate of the unquantized ARMA error ζ_{yt}^* in (20a). The following proposition shows this can be achieved.

Theorem 1. *Consider the ARMA$_K$ graph filter of order K in* (16) *with coefficients $\boldsymbol{\Psi}$ and $\boldsymbol{\varphi}$, and quantization error $\boldsymbol{\epsilon}_{yt}^q$. Let $\psi_{max}=max(|\psi_1|,|\psi_2|,\cdots,|\psi_K|)$ be the ARMA$_K$ coefficient with largest magnitude and let all ARMA$_K$ branches be stable i.e., $\psi_{max}\lambda_{max}<1$ for all $k=1\cdots K$. Consider also that the signal is quantized with a uniform quantizer with a decreasing stepsize over the iterations t as $\Delta_t=(\psi_{max}\lambda_{max})^t\Delta_0$. The quantization MSE ζ_{yt}^q of the filter output at iteration t is upper bounded by:*

$$\zeta_{yt}^q \leq \frac{K\Delta_0}{12}t(\psi_{max}\lambda_{max})^{2t} \tag{24}$$

which at the steady-state converges to zero ($\zeta_{yt\to\infty}^q\to 0$) at a rate of $t(\psi_{max}\lambda_{max})^{2t}$.

Proof: See Appendix VIII-F. □

Theorem 1 shows the advantage of adopting a decreasing quantization stepsize, which leads to vanishing the quantization MSE for the ARMA filters at the steady-state. This behavior is similar to the convergence error of the unquantized

ARMA ζ_{yt}^* and suggests that at the steady-state, we can reach the designed filter response. However, the quantization MSE converges with a rate $t(\psi_{\max}\lambda_{\max})^{2t}$ instead of $(\psi_{\max}\lambda_{\max})^{2t}$. Faster convergence rates can be achieved by decreasing the quantization stepsize at a faster rate over time but this requires transmitting more bits for larger values of t.

Despite vanishing the quantization MSE at the steady-state, the dynamic quantization stepsize comes together with a cost. In particular, for large values of t, this implies that the quantization stepsize becomes infinitesimal; hence, the number of bits transmitted per iteration becomes that of the conventional ARMA graph filter [cf. (5)] after some iteration numbers $t \geq t^*$. Nevertheless, this strategy reduces the communication efforts in the first iterations, i.e., we can start with a coarser Δ_0. For b_t being the number of bits transmitted at iteration t, the communication cost of the ARMA$_K$ graph filter per iteration is of order $\mathcal{O}(MKb_t)$. If b is the average number of bits transmitted over $t_{\max}$ iterations, the ARMA$_K$ communication complexity is of order $\mathcal{O}(MKt_{\max}b)$. The benefits of following this approach is that the ARMA design is readily available from the unquantized setting [11].

A related problem that can be of interest is to find the best sequence of quantization stepsizes $\Delta_0, \Delta_1, \cdots, \Delta_t$ by taking into account the constraints of a given total bit budget $\mathcal{B}$ available and a maximum number of iterations $t_{\max}$, where $\Delta_t = (\psi_{\max}\lambda_{\max})^t\Delta_0$. Note that the quantization stepsize Δ_t is defined as the ratio of the quantization range r_t at iteration t over the number of quantization intervals, which is given by $\Delta_t = r_t/2^{b_t} = (x_{\text{upp}} - x_{\text{low}})/2^{b_t}$. Thus, the best sequence of quantization stepsizes can be obtained for $\psi_{\max}\lambda_{\max} \neq 0$ and $\psi_{\max}\lambda_{\max} < 1$ by solving the problem $\sum_{t=0}^{t_{\max}} \log_2\left(\frac{(x_{\text{upp}}-x_{\text{low}})}{(\psi_{\max}\lambda_{\max})^t\Delta_0}\right) = \mathcal{B}$, which implies:

$$\Delta_0 = 2^{\left(-\frac{\mathcal{B}}{1+t_{\max}}\right)}\,(x_{\text{upp}} - x_{\text{low}})\,(\psi_{\max}\lambda_{\max})^{-\frac{t_{\max}}{2}} \tag{25}$$

V. Quantization analysis over time-varying graphs

We now extend the quantization analysis to cases where the graph connectivity changes randomly over the filtering iterations. This scenario is expected to occur in applications of graph filtering over WSNs. For our analysis, we consider directly the more general dynamically decreasing quantization stepsize and the random edge sampling model from [26].

Definition 1 (Random edge sampling model [26])**.** *Consider an underlying graph $\mathcal{G} = (\mathcal{V}, \mathcal{E})$. A random edge sampling (RES) graph realization $\mathcal{G}_t = (\mathcal{V}, \mathcal{E}_t)$ of $\mathcal{G}$ is composed of the same set of nodes $\mathcal{V}$ and a random set of links $\mathcal{E}_t \subseteq \mathcal{E}$ that are activated (i.e., $(i,j) \in \mathcal{E}_t$) with a probability p_{ij} ($0 < p_{ij} \leq 1$). The links are activated independently over the graph and time and are mutually independent from the graph signal.*

We consider the RES graph realization to model the link losses that occur at each filter iteration. As such, the RES model states that the realization $\mathcal{G}_t = (\mathcal{V}, \mathcal{E}_t)$ at iteration t is drawn from the underlying connectivity graph $\mathcal{G} = (\mathcal{V}, \mathcal{E})$, where the links $\mathcal{E}_t \subseteq \mathcal{E}$ are generated via an i.i.d. Bernoulli process with probability p_{ij}. Let then $\mathbf{P} \in \mathbb{R}^{N\times N}$ denote the matrix that collects the link activation probabilities p_{ij}. Let also $\mathbf{S}$, $\mathbf{S}_t$, and $\bar{\mathbf{S}}$ denote, respectively, the shift operator of the underlying graph $\mathcal{G}$, the graph realization $\mathcal{G}_t$ at iteration t, and the expected graph $\bar{\mathcal{G}}$. Since graph $\mathcal{G}$ has an upper bounded shift operator $\|\mathbf{S}\|_2 \leq \rho$, all its realizations $\mathcal{G}_t$ have also an upper bounded shift operator $\|\mathbf{S}_t\|_2 \leq \|\mathbf{S}\|_2 \leq \rho$ [52], [53].

Before, we proceed with the filter analysis, the following remark is in order. Under the RES model, if $\mathbf{S} = \mathbf{A}$ then the expected shift operator is $\bar{\mathbf{S}} = \mathbb{E}[\mathbf{A}_t] = \mathbf{P} \circ \mathbf{A}$. If $\mathbf{S} = \mathbf{L}$, then the expected shift operator[4] is $\bar{\mathbf{S}} = \mathbb{E}[\mathbf{L}_t] = \bar{\mathbf{D}} - (\mathbf{P} \circ \mathbf{A})$, where $\bar{\mathbf{D}} = \mathbb{E}[\mathbf{D}_t]$ is a diagonal matrix whose non zero entries are given by $[\bar{\mathbf{D}}]_{ii} = \sum_{j=1}^N a_{ij}p_{ij}$.

A. FIR graph filters

When the FIR filter is run over RES graph realizations, the instantaneous shift operator $\mathbf{S}_t$ is present in the filtering expression (2) and affects the output. To characterize this output, let us define the transition matrix of the RES graph realisations $\mathcal{G}_t, \ldots, \mathcal{G}_{t'}$, $\mathbf{\Theta}(t',t) = \prod_{\tau=t}^{t'} \mathbf{S}_\tau$ if $t' \geq t$ and $\mathbf{I}$ if $t' < t$. The FIR filter output over a sequence of K time-varying graphs is:

$$\mathbf{y}_t = \sum_{k=0}^{K} \phi_k\, \mathbf{\Theta}(t-1, t-k)\, \mathbf{x} \tag{26}$$

where the filter output is computed by considering all graph realizations from the iteration $t-K$ to t. From the independence of RES graph realizations, the expected FIR output is:

$$\bar{\mathbf{y}}_t = \mathbb{E}\big[\mathbf{y}_t\big] = \sum_{k=0}^{K} \phi_k \bar{\mathbf{S}}^k \mathbf{x}. \tag{27}$$

As shown in Appendix VIII-G, the quantized FIR filter output over RES graph realizations can be written as $\mathbf{y}_t^{\text{q}} = \mathbf{y}_t + \boldsymbol{\epsilon}_t$ where the quantization error $\boldsymbol{\epsilon}_t$ has the expression:

$$\boldsymbol{\epsilon}_t = \sum_{k=1}^{K}\sum_{\kappa=0}^{k-1} \phi_k \mathbf{\Theta}(t-\kappa-1, t-k)\, \mathbf{n}_{\text{q}}^{(\kappa)}. \tag{28}$$

The latter accounts for the percolation of the quantization noise $\mathbf{n}_{\text{q}}^{(\kappa)}$ over different random graph realizations. Since the quantization noise has a zero mean, the expected FIR output with quantization is $\mathbb{E}\big[\mathbf{y}_t^{\text{q}}\big] = \bar{\mathbf{y}}_t$ [cf. (27)]. That is, in expectation, the FIR graph filter behaves as the filter in (26) operating on the expected graph with unquantized data.

To quantify the statistical impact of the quantization noise, we analyze the second order moment of the quantized output $\mathbf{y}_t^{\text{q}}$ in the following proposition.

Proposition 4. *Consider the FIR graph filter operating over the RES graph realizations $\mathcal{G}_t$ [cf. Def. 1] with shift operators $\mathbf{S}_t$ upper bounded as $\|\mathbf{S}_t\|_2 \leq \rho$. Let also the filter input signal be quantized with a dynamic quantization stepsize Δ_t at iteration t. The MSE of the filter output due to quantization and graph randomness $\zeta_t^{\text{q}} = \mathbb{E}[\frac{1}{N}tr(\boldsymbol{\epsilon}_t\boldsymbol{\epsilon}_t{}^H)]$ is upper bounded by:*

$$\zeta_t^q \leq \frac{1}{12}\sum_{\kappa=1}^{K} \Delta_{\kappa-1}^2 \left(\sum_{k=\kappa}^{K} \rho^{k-\kappa+1}|\phi_k|\right)^2. \tag{29}$$

Proof: See Appendix VIII-H. □

[4]Note that if $\mathbf{P}$ has equal rows so that $p_{ij} = p_i$ for all $j \in \mathcal{V}$ or has equal entries i.e. $p_{ij} = p$, we have $\mathbb{E}[\mathbf{L}_t] = \mathbf{P} \circ \mathbf{L}$.

Note that Proposition 4 represents the worst-case bound for the graph randomness. This is similar to the unquantized graph filters over RES graphs [26] because the spectral radius ρ accounts for all potential link losses (it is independent on the probabilities p_{ij}). On the other hand, this result serves as a proxy for the MSE to design a graph filter that is robust to both link losses and quantization error.

Filter design. Our goal is to design the filter coefficients $\phi_0, \ldots, \phi_K$ to reduce the quantization MSE in (29) while keeping the quantized graph filter output $\mathbf{y}_t^{\mathrm{q}}$ close in expectation to the unquantized output over the deterministic graph $\mathcal{G}$; we denote the latter as $\mathbf{y}^{\diamond} = \sum_{k=0}^{K} \phi_k^{\diamond} \mathbf{S}^k \mathbf{x}$. Then, let us consider the expected error due to quantization (bias):

$$\bar{\mathbf{e}} = \mathbb{E}\big[\mathbf{y}_t^{\mathrm{q}} - \mathbf{y}^{\diamond}\big] = \mathbb{E}\big[\mathbf{y}_t^{\mathrm{q}}\big] - \mathbf{y}^{\diamond}. \tag{30}$$

While we can design the coefficients to minimize this bias, they will not account for the deviation around it. Therefore, we consider the more involved problem of finding the filter coefficients as a trade-off between the expected error of the filter output and the quantization MSE. For this, let us define the filtering matrix difference $\bar{\mathbf{E}}$:

$$\bar{\mathbf{E}} = \sum_{k=0}^{K} \big(\phi_k \, \bar{\mathbf{S}}^k - \phi_k^{\diamond} \, \mathbf{S}^k\big) \tag{31}$$

that accounts for the response difference between the graph filtering over the expected graph $\bar{\mathcal{G}}$ and the graph filtering over the deterministic graph $\mathcal{G}$. Then, we find the filter coefficients by solving the convex problem:

$$\underset{\phi_k}{\text{minimize}} \, \big\|\bar{\mathbf{E}}\big\|_F + \frac{\gamma}{12} \sum_{\kappa=1}^{K} \Delta_{\kappa-1}^2 \bigg(\sum_{k=\kappa}^{K} \rho^{k-\kappa+1} |\phi_k| \bigg)^2 \tag{32}$$

where $\|\bar{\mathbf{E}}\|_F$ is the Frobenius norm of (31) and γ is a weighting factor trading-off the expected error and quantization MSE.

B. ARMA graph filters

The parallel ARMA filter operating over random graphs has the branches outputs:

$$\mathbf{w}_t = (\boldsymbol{\Psi} \otimes \mathbf{S}_{t-1}) \mathbf{w}_{t-1} + \boldsymbol{\varphi} \otimes \mathbf{x} \tag{33}$$

which in the presence of quantization noise becomes:

$$\mathbf{w}_t^{\mathrm{q}} = (\boldsymbol{\Psi} \otimes \mathbf{S}_{t-1})(\mathbf{w}_{t-1}^{\mathrm{q}} + \mathbf{n}_{t-1}^{\mathrm{q}}) + \boldsymbol{\varphi} \otimes \mathbf{x}. \tag{34}$$

By expanding (34) to all the terms, we can write the overall ARMA filter output due to quantization as:

$$\begin{aligned} \mathbf{w}_t^{\mathrm{q}} &= \Big(\prod_{\tau=0}^{t-1} \boldsymbol{\Psi} \otimes \mathbf{S}_{\tau}\Big) \mathbf{w}_0 + \boldsymbol{\varphi} \otimes \mathbf{x} + \sum_{\tau=1}^{t-1} \bigg(\prod_{\tau'=t-\tau}^{t-1} \boldsymbol{\Psi} \otimes \mathbf{S}_{\tau'} \bigg) (\boldsymbol{\varphi} \otimes \mathbf{x}) + \boldsymbol{\varepsilon}_t^{\mathrm{q}} \\ \mathbf{y}_t^{\mathrm{q}} &= (\mathbf{1}^{\top} \otimes \mathbf{I}_N) \mathbf{w}_t^{\mathrm{q}} \end{aligned} \tag{35}$$

where in order to ease notation, we have denoted by $\boldsymbol{\varepsilon}_t^{\mathrm{q}} = \sum_{\tau=0}^{t-1} \big(\prod_{\tau'=\tau}^{t-1} \boldsymbol{\Psi} \otimes \mathbf{S}_{\tau'} \big) \mathbf{n}_{\tau}^{\mathrm{q}}$ the percolation of the quantization noise $\mathbf{n}_{\tau}^{\mathrm{q}}$ over the parallel ARMA branches up to time t. Then, let us consider the filter output error $\boldsymbol{\varepsilon}_{yt} = \mathbf{y}_t^{\mathrm{q}} - \mathbf{y}^*$ from the steady-state expected ARMA output $\mathbf{y}^*$:

$$\boldsymbol{\varepsilon}_{yt} = \boldsymbol{\varepsilon}_{yt}^{\mathrm{q}} + \boldsymbol{\varepsilon}_{yt}^* \tag{36}$$

where $\boldsymbol{\varepsilon}_{yt}^{\mathrm{q}} = (\mathbf{1}^{\top} \otimes \mathbf{I}_N) \boldsymbol{\varepsilon}_t^{\mathrm{q}}$ is the quantization error on the output; $\boldsymbol{\varepsilon}_{yt}^* = (\mathbf{1}^{\top} \otimes \mathbf{I}_N) \boldsymbol{\varepsilon}_t^*$ is the unquantized ARMA graph filter error at iteration t w.r.t. to its steady-state $\mathbf{y}^*$. Then, let us denote by $\boldsymbol{\varepsilon}_t^*$ the unquantized ARMA error w.r.t. to the steady-state $\mathbf{w}^*$, which is given by:

$$\boldsymbol{\varepsilon}_t^* = \bigg(\prod_{\tau=0}^{t-1} \boldsymbol{\Psi} \otimes \mathbf{S}_{\tau}\bigg) \mathbf{w}_0 + \boldsymbol{\varphi} \otimes \mathbf{x} + \sum_{\tau=1}^{t-1} \bigg(\prod_{\tau'=t-\tau}^{t-1} \boldsymbol{\Psi} \otimes \mathbf{S}_{\tau'} \bigg) (\boldsymbol{\varphi} \otimes \mathbf{x}) - \mathbf{w}^*. \tag{37}$$

Under the RES graph model and given the zero-mean quantization noise, it can be easily shown from (33) and (34) that $\mathbb{E}[\mathbf{w}_t^{\mathrm{q}}] = \mathbb{E}[\mathbf{w}_t]$; i.e., in expectation both the quantized and unquantized ARMA filters give the same output. However, the quantization impacts on the second order moment of the filter output error $\boldsymbol{\varepsilon}_{yt}$ in (36). We analyze next the MSE of the latter, which by simple algebra, can be split as:

$$\xi_{yt} = \frac{1}{N} \mathbb{E}[\mathrm{tr}(\boldsymbol{\varepsilon}_{yt} \boldsymbol{\varepsilon}_{yt}^{\mathrm{H}})] = \xi_{yt}^* + \xi_{yt}^{\mathrm{q}}. \tag{38a}$$

where:

$$\xi_{yt}^* = \frac{1}{N} \mathbb{E}[\mathrm{tr}((\mathbf{1}^{\top} \otimes \mathbf{I}_N) \boldsymbol{\varepsilon}_t^* (\boldsymbol{\varepsilon}_t^*)^{\mathrm{H}} (\mathbf{1}^{\top} \otimes \mathbf{I}_N)^{\mathrm{H}})] \tag{38b}$$

$$\xi_{yt}^{\mathrm{q}} = \frac{1}{N} \mathbb{E}[\mathrm{tr}((\mathbf{1}^{\top} \otimes \mathbf{I}_N) \boldsymbol{\varepsilon}_t^{\mathrm{q}} (\boldsymbol{\varepsilon}_t^{\mathrm{q}})^{\mathrm{H}} (\mathbf{1}^{\top} \otimes \mathbf{I}_N)^{\mathrm{H}})] \tag{38c}$$

and where we have used the linearity of the expectation w.r.t the trace, the cyclic property of the trace, and the independence of $\mathbf{x}$, $\mathbf{w}_0$ and $\mathbf{n}_{\tau}^{\mathrm{q}}$. ξ_{yt}^* is the MSE for the case of unquantized filter w.r.t. to its steady-state output. The next Theorem provides an upper bound on the MSE of the filter output due to quantization and graph randomness ξ_{yt}^{q}, when the quantization stepsize Δ_t decreases at each iteration t.

Theorem 2. *Consider the ARMA$_K$ graph filter operating over RES graph realizations $\mathcal{G}_t$ [cf. Def. 1] with shift operators $\mathbf{S}_t$ upper bounded as $\|\mathbf{S}_t\|_2 \leq \rho$. Let $\psi_{max} = max(|\psi_1|, |\psi_2|, \cdots, |\psi_K|)$ be the ARMA$_K$ coefficient with largest magnitude and let all ARMA$_K$ branches be stable i.e., $\psi_{max} \ \rho < 1$ for all $k = 1 \cdots K$. Let also the filter input signal be quantized with a uniform quantizer having a stepsize decreasing over the iterations t as $\Delta_t = (\psi_{max} \, \rho)^t \Delta_0$. The MSE of the ARMA filter output at iteration t due to quantization and graph randomness ξ_{yt}^q can be upper bounded by:*

$$\xi_{yt}^q \leq \frac{K^2 \, \Delta_0}{12} t \, (\psi_{max} \, \rho)^{2t} \tag{39}$$

making the quantization MSE converge to zero ($\xi_{yt \to \infty}^q \to 0$) at a rate of $t(\psi_{max} \, \rho)^{2t}$.

Proof: See Appendix VIII-I. □

Theorem 2 highlights that the quantization MSE converges to zero when using a decreasing quantization stepsize, despite the random topological changes and the presence of quantization. This implies that there is no need to consider the quantization MSE in the design phase. However, contrarily to time-invariant graphs, the overall MSE of ARMA filters, which is affected by both the quantization ξ_{yt}^{q} and the random variation part ξ_{yt}^*, can not reach the desired filter response at steady-state ($t \to \infty$), because even if the quantization MSE ξ_{yt}^{q} can be made to converge to zero, the unquantized MSE ξ_{yt}^* does not converge to zero due to graph topological changes.

Similarly to time-invariant graphs in Section IV-B, where we consider the constraints of a given total bit budget $\mathcal{B}$ available and a maximum number of iterations $t_{\max}$, the

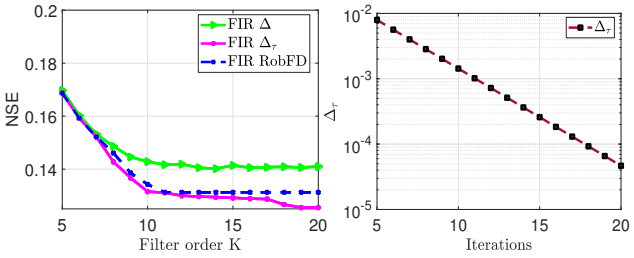

(a) (b)

Fig. 1. (a) NSE of FIR graph filters over time-invariant graphs, when approximating an ideal low-pass filter. The filter coefficients are optimized by solving (15), where $N = 200$, $a_s = 220$ m, $\mathbf{S} = 0.5\mathbf{L}_{\text{n}}$, $\Delta_0 = 0.044$ and $\chi = 32$ bits. FIR filters with fixed stepsize (FIR Δ in green) and decreasing stepsize (FIR Δ_τ in pink) are compared to the Robust Filter Design (RobFD) proposed in [35]. (b) Decreasing quantization stepsize over iterations is given by $\Delta_\tau = (0.71)^\tau \Delta_0$ for $b_\tau \leq \chi$.

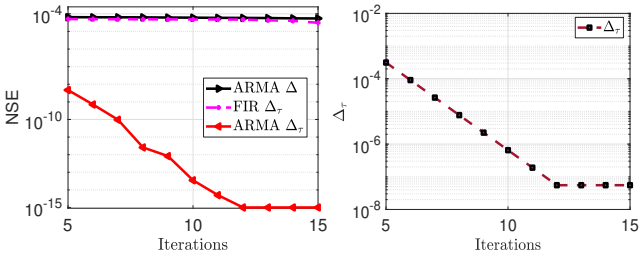

(a) (b)

Fig. 2. (a) NSE between the quantized output and the unquantized output of FIR and ARMA filtering over time-invariant graphs for the Tikhonov denoising problem, where $N = 10000$, $a_s = 2200$ m, $\mathbf{S} = \lambda_{\max}^{-1}\mathbf{L}$ and $w = 0.3$, $\psi_{\max}\lambda_{\max} = 0.3$. The FIR filter coefficients are optimized by solving (15), with $\Delta_0 = 0.15$ and $\chi = 25$ bits. The x-axis is the number of iterations for the ARMA$_1$ filter, while for the FIR filter "Iterations = K". (b) Decreasing quantization stepsize over iterations is given by $\Delta_\tau = (0.3)^\tau \Delta_0$ for $b_\tau \leq \chi$.

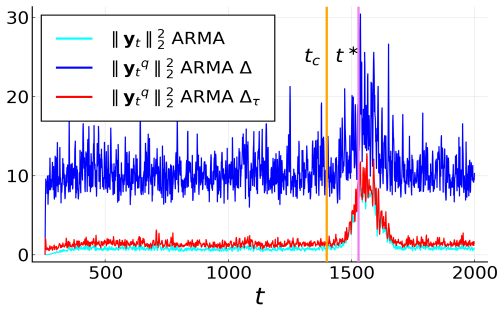

Fig. 3. Squared norm of unquantized and quantized filtered streaming graph signals for the change point detection problem, when using the ARMA$_4$ filter of NOUGAT algorithm [54], where $N = 200$, $a_s = 300$ m, $\mathbf{S} = \mathbf{L}_{\text{n}} - \mathbf{I}$, $\Delta_0 = 1.19$, $\chi = 5$ bits. The change-point is set at $t_c = 1400$ and the NOUGAT detection is expected at $t^* = t_c + 128$ for the same NOUGAT parameter values of [54].

best sequence of quantization stepsizes is given by $\Delta_0 = 2^{\left(-\frac{\mathcal{B}}{1+t_{\max}}\right)} (\psi_{\max}\rho)^{-\frac{t_{\max}}{2}} (x_{\text{upp}} - x_{\text{low}})$ and $\Delta_t = (\psi_{\max}\,\rho)^t \Delta_0$, for $\psi_{\max}\,\rho \neq 0$ and $\psi_{\max}\,\rho < 1$.

Corollary 2.1. *Consider same settings as Theorem 2 with the input signal quantized with a uniform quantizer having a fixed quantization stepsize Δ. The MSE of the filter output due to quantization and graph randomness ξ_{yt}^q can be upper bounded by:*

$$\xi_{yt}^q \leq K^2\sigma_q^2 \frac{(\psi_{max}\,\rho)^2 - [(\psi_{max}\,\rho)^2]^{t+1}}{1-(\psi_{max}\,\rho)^2} \tag{40}$$

which in the steady-state ($t \to \infty$) becomes:

$$\xi_{yt\to\infty}^q \leq K^2\sigma_q^2 \frac{(\psi_{max}\,\rho)^2}{1-(\psi_{max}\,\rho)^2} \tag{41}$$

Proof. By considering a fixed quantization stepsize Δ, the upper bound of the MSE of ARMA filter due to quantization and graph randomness in (76) becomes:

$$\xi_{yt}^{\text{q}} \leq K^2\sigma_{\text{q}}^2 \sum_{\tau=1}^{t} \left(\psi_{\max}\,\rho\right)^{2\tau} \tag{42}$$

By considering the upper bound in (42) is finite geometric series with argument smaller than 1, ξ_{yt}^{q} can be upper bounded by (40). □

VI. Numerical Experiments

This section corroborates our theoretical findings with numerical experiments on both synthetic and real data from the NOAA [55] and the Intel Berkely sensor network [56].

A. Synthetic data

We consider up to $N = 10000$ sensor nodes, which are randomly and uniformly distributed over a square area of side a_s. Each node can communicate with the neighbors within the transmission range $R = 50$ m. The latter forms a communication network that can be used to perform distributed graph filtering operations. In the sequel, we evaluate our quantized filtering designs in three different applications: baseline ideal-low pass filter, signal denoising, and change-point detection. To account for the graph randomness, we average the results over 1000 different realizations. The FIR filter coefficients are optimized by solving (15) or (32) for time-invariant and time-varying graphs, respectively.

Ideal low-pass filter. We consider the FIR graph filter to approximate an ideal low-pass filter with frequency response $h(\lambda) = 1$ if $\lambda \leq \lambda_c$ and zero otherwise. The shift operator is $0.5\mathbf{L}_{\text{n}}$. The cut off frequency λ_c is half the spectrum. The input signal $\mathbf{x}$ is such that its GFT is all one.

Fig. 1 (a) shows the Normalized Squared Error NSE $= \|\hat{\mathbf{y}}^{\text{q}} - \hat{\mathbf{y}}\|_2^2 / \|\hat{\mathbf{y}}\|_2^2$ between the quantized output $\hat{\mathbf{y}}^{\text{q}}$ and the unquantized desired signal $\hat{\mathbf{y}}$ in the graph frequency domain, when the FIR filters run over time-invariant graphs. The quantization stepsize Δ_k is limited through χ, which restricts the maximum number of bits used at each iteration. The results show that both our designed FIR graph filters and the Robust Filter Design (RobFD) [35] achieve similar performance for low filter orders ($K < 8$). However, the FIR graph filter with decreasing quantization stepsize performs better than the other two alternatives for higher filter orders. The theoretical MSE upper-bounds of FIR filters, computed by using (13) for fixed stepsize and using (14) for a decreasing stepsize, are $4.49\ 10^{-1}$ and $3.49\ 10^{-1}$, respectively. These upper-bounds are in concordance with our simulated results obtained in Fig. 1 (a).

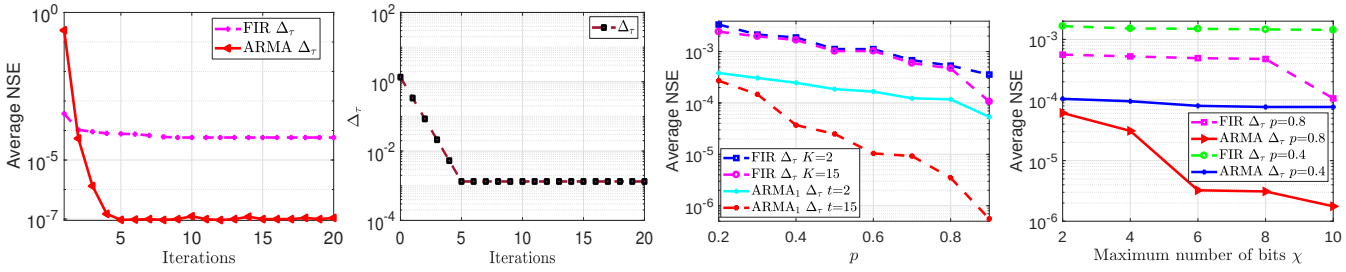

(a) $p = 0.95$, $\chi = 15$ bits (b) $\chi = 15$ bits (c) $\chi = 15$ bits (d) 10 iterations

Fig. 4. (a)(c)(d) Average NSE between the quantized output over time-varying graph and the unquantized output over a deterministic graph for both FIR and ARMA filters for the Tikhonov denoising problem, where $N = 10000$, $a_s = 2200$ m, $\mathbf{S} = \lambda_{\max}^{-1}\mathbf{L}$, $w = 0.25$, $\Delta_0 = 1.36$ and $\psi_{\max}\rho = 0.25$. The FIR filter coefficients are optimized by solving (32). (a) Average NSE vs. iterations, where $p = 0.95$ and $\chi = 15$ bits. The x-axis is the number of iterations for the ARMA$_1$ filter, while for the FIR filter "Iterations = K". (b) Decreasing quantization stepsize over iterations is given by $\Delta_\tau = (0.25)^\tau \Delta_0$ for $b_\tau \leq \chi$. (c) Average NSE vs. the probability p of link activation, where $\chi = 15$ bits. (d) Average NSE vs. the maximum number of bits χ at each iteration, where $K = 10$ for FIR filter and $t = 10$ for ARMA$_1$ filter.

Tikhonov denoising. We now evaluate the performance of the proposed solutions in distributed denoising. We assume a noisy graph signal $\mathbf{x} = \mathbf{z} + \mathbf{n}$, where $\mathbf{z}$ is the signal of interest and $\mathbf{n}$ is a zero mean additive noise. To recover signal $\mathbf{z}$, we solve the Tikhonov denoising problem:

$$\mathbf{z}^* = \underset{\mathbf{z}\in\mathbb{R}^N}{\operatorname{argmin}} \|\mathbf{x} - \mathbf{z}\|_2^2 + w\, \mathbf{z}^\top \mathbf{S}\mathbf{z} \tag{43}$$

for $\mathbf{S} = \mathbf{L}$ or $\mathbf{S} = \mathbf{L}_{\text{n}}$ and where the regularizer $\mathbf{z}^\top\mathbf{S}\mathbf{z}$ is based on the prior assumption the graph signal varies smoothly with respect to the underlying graph and w is the weighting factor trading smoothness and noise removal [2]. The closed-form solution of (43) is an ARMA$_1$ filter $\mathbf{z}^* = (\mathbf{I} + w\mathbf{S})^{-1}\mathbf{z}$ with coefficients $\psi = -w$ and $\varphi = 1$ [11]. Hence, we can employ the ARMA$_1$ filter to solve distributively the Tikhonov denoising problem.

In Fig. 2 (a), we compare the NSE$= \|\mathbf{y}_t^{\text{q}} - \mathbf{y}_t\|_2^2/\|\mathbf{y}_t\|_2^2$ between the quantized and the unquantized outputs of FIR and ARMA graph filters over time-invariant graphs. We use a normalized shift operator[5] $\mathbf{S} = \lambda_{\max}^{-1}\mathbf{L}$. The noise in this instance is zero-mean Gaussian with variance $\sigma^2 = 0.2$. The theoretical MSE upper-bounds of ARMA, computed by using (21) for fixed stepsize and using (24) for a stepsize decreasing over twelve iterations, are respectively $2.33\ 10^{-3}$ and $4.23\ 10^{-14}$. Once again, these upper-bounds are in concordance with our simulated results obtained in Fig. 2 (a). We observe also the ARMA graph filter with decreasing quantization stepsize significantly outperforms both the ARMA with fixed quantization stepsize and the FIR graph filter with optimized filter coefficients and decreasing quantization stepsize. The latter corroborates our finding in Theorem 1: ARMA filters reach machine precision with a decreasing quantization stepsize.

We now evaluate the filters over time-varying graphs, by analyzing the average NSE between the quantized output over the time-varying graph $\mathbf{y}_t^{\text{q}}$ and the unquantized output $\mathbf{y}_t$ over the deterministic graph. As shown in Fig. 4 (a), the ARMA graph filter presents significantly better performance than the FIR graph filter, when the link activation probability is $p = 0.95$ and the quantization stepsize is decreasing over the iterations. This is because the quantization MSE with ARMA converges to zero when using a decreasing quantization stepsize, as stated in Theorem 2. This also explains why we observe that the average NSE for ARMA filters reduces considerably when the number of iterations increases. Notice also that the NSE floor of the ARMA filter is the value when the signal is quantized with all the available bits and where Δ_τ is very small. The latter corresponds to the machine precision accuracy, corroborating our results in Theorem 2. The theoretical MSE upper-bounds computed with (29) and (39) respectively for FIR and ARMA, when the stepsize is decreased over the five first iterations, are $1.17\ \ 10^{-3}$ and $5.41\ \ 10^{-7}$. These upper-bounds are in a total concordance with the results obtained in Fig. 4 (a).

In Figs. 4 (c)-(d), we analyze the average NSE for different probabilities of link activation and different maximum numbers of bits used for quantization. ARMA filters with decreasing quantization stepsize achieves always the highest filtering accuracy with a significant margin compared to other filters due to the convergence of its quantization MSE to zero, as shown in Theorem 2. Fig. 4 (c) shows that, as expected, better link connectivities (higher p) lead to lower errors. It is also worth noticing that the graph filtering accuracy is less affected by topological changes (due to link losses) for lower filter orders K\number of iterations t, as compared to higher filter orders\iterations. This is because the exchanges between nodes through problematic links reduce. This highlights the trade-off between the filter order\iteration number and the robustness to topological changes. In a highly stable topology, a higher filter order\iteration number improves the graph filtering accuracy. Fig. 4 (d) shows that the average NSE decreases when the maximum number of bits used for quantization at each iteration is higher. This is because increasing the quantization bits decreases the quantization stepsize at each iteration, which reduces as well the quantization errors accumulated among iterations. We can also observe that increasing the quantization bits does not lead necessarily to a noticeable improve of the filtering accuracy, especially for low probability of link activation, as compared to higher probability of link activation. We attribute this behavior to the large number of links that fall, therefore, the error due to link losses dominates that of quantization.

[5]This improves the stability of the ARMA filter and ensures a small spectral radius bound that can reduce the filtering and the quantization error.

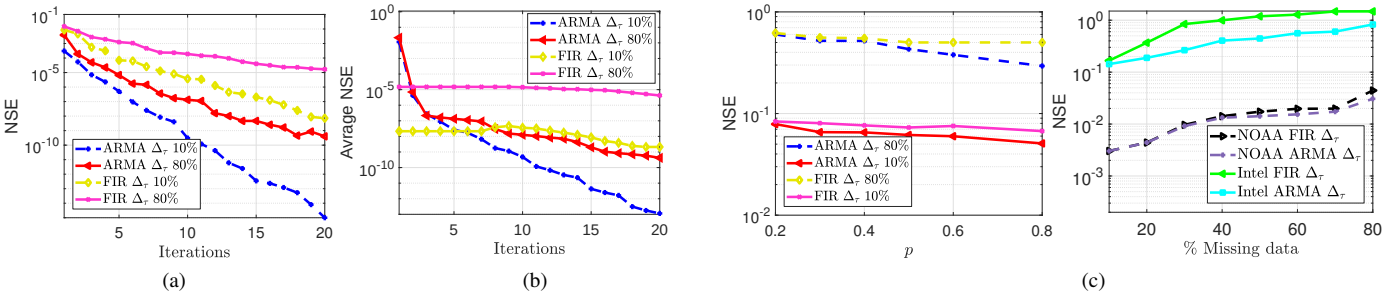

Fig. 5. (a) NSE between the quantized output and the unquantized output of graph filters, when interpolating the missing temperature values in NOAA data set and where $\Delta_0 = 3.18$ and $\mathbf{S} = \mathbf{L}_{\text{n}}$. The FIR filter coefficients are optimized by solving (15). (b) Average NSE between the quantized output and the unquantized output of graph filters, when interpolating the missing light values in Intel Lab data set and where $\Delta_0 = 0.7$ and $\mathbf{S} = \lambda_{\max}^{-1}\mathbf{L}$. The FIR filter coefficients are optimized by solving (32). (a)-(b) The x-axis is the number of iterations for ARMA_1 filter while for FIR filter "Iterations = K". (c) NSE between the quantized output and the graph signal to be reconstructed. Here, we plot NSE vs. probability of link activation p for Intel data, where $\Delta_0 = 5.3$ and 10 iterations (left), and NSE vs. % missing data for different data sets and 20 iterations (right). (a)(b)(c) Parameters are $w = 0.3$ and $\chi = 15$ bits.

Change-point detection. We now evaluate the performance of the proposed solutions in the application of change point detection of streaming graph signals. The change-point detection aims to localize the switching time instant from which the statistical properties of a signal change. This problem can be solved distributively by using the NOUGAT algorithm [54], which performs an ARMA_K filter. Based on NOUGAT algorithm steps, a point-change can be detected if the squared norm of the filtered streaming graph signal is higher than a certain threshold. Fig. 3 illustrates the detection performance by comparing the squared norm of unquantized and quantized graph filter outputs. The change-point is set at $t_c = 1400$, and given window lengths of 128 samples, the NOUGAT detection is expected at $t^* = t_c + 128$. It can be clearly seen that by using an ARMA_4 with decreasing quantization stepsizes, the detection performance is very close to the unquantized case. Moreover, the change-point is better localized as compared to the case of fixed quantization stepsize.

B. Real data

We now illustrate the performance of the proposed solutions for the graph signal interpolation task over time-invariant and time-varying topologies with two real data sets.

NOAA data set. This data set contains hourly observations of temperature measurements of N=109 stations collected in the United States in 2010 [55], for a total of 8759 hours. We use the same graph structure as [13], which is built from the nodes coordinates by using the default 7-NN nearest neighbor. The graph signal at node i is the temperature value at i-th station.

Let $\mathbf{x}'$ be the observed graph signal $\mathbf{x}$ with missing values. We aim at reconstructing the overall graph signal $\mathbf{x}$ from the observations $\mathbf{x}'$ by exploiting the smoothness of $\mathbf{x}$ over the graph. This problem can be formulated as [57], [58]:

$$\mathbf{x}^\star = \underset{\mathbf{x}\in\mathbb{R}^N}{\text{argmin}} \|\mathbf{T}(\mathbf{x}-\mathbf{x}')\|_2^2 + w\ \mathbf{x}^\top\mathbf{S}\mathbf{x} \qquad (44)$$

where $\mathbf{T}$ is a diagonal matrix with $\mathbf{T}_{ii} = 1$ if x_i is known and $\mathbf{T}_{ii} = 0$ otherwise and w is the weighting factor. The optimal solution of the convex optimization problem (44) is $\mathbf{x}^\star = (\mathbf{T} + w\mathbf{S})^{-1}\mathbf{x}' = (\mathbf{I} - \tilde{\mathbf{S}})^{-1}\mathbf{x}'$, which is an ARMA_1 filter for the shift operator $\tilde{\mathbf{S}} = \mathbf{T} + w\mathbf{S} - \mathbf{I}$ [11]. To generate missing values in the NOAA data set, we randomly remove signal values with a certain percentage. Then, we analyze the NSE between the quantized output and the unquantized output of graph filters, for different percentages of missing values.

Fig. 5 (a) shows the NSE decreases considerably at each iteration, particularly for ARMA filters. It is also worth noticing this decrease enhances when less data are missing.

Intel Lab data set. The Intel Berkeley Research Lab data set contains light data of $N = 54$ Mica2Dot sensor nodes distributed in an indoor environment over an area of 1200 m^2 [56]. The communication between the sensor nodes is wireless and prone to channel noise and interference, leading to time-varying graph topological changes due to link losses [59]. The probability of link activation of the nodes is about 0.13 with a standard deviation of 0.18. The underlying graph topology has high connectivity with an average node degree of 47, implying multiple communication paths exist between nodes, helping to make signal exchanged between nodes robust to link losses. The graph signal at node i is the light value at i-th sensor. We perform graph signal interpolation to reconstruct the missing light values.

In Fig. 5 (b), we analyze the average quantized NSE as a function of the missing values for the FIR and ARMA graph filters. Even though the graph filtering accuracy is affected by the accumulated quantization errors over iterations and the graph topological changes, ARMA filters provide a significant decrease in terms of NSE, when the number of iterations grows and the percentage of missing data is low. Notice that in practical settings with decreasing quantization stepsizes over time-varying graphs, it is preferable to use FIR graph filters for low filter orders. However, for large filter orders\iterations, ARMA graph filters are the best choice since they provide better performance than FIR filters, and the quantization MSE can be significantly decreased.

Fig. 5 (c) (left) represents the NSE between the quantized graph signal output and the true signal for the Intel lab data as a function of the probability of link activation p. As expected, better link connectivities lead to lower graph filtering errors and better signal reconstruction, especially with ARMA filters. Fig. 5 (c) (right) depicts the NSE between the quantized graph signal output and the true signal for the two data sets as a function of the missing values. The results show that for both

data sets a good performance in terms of signal reconstruction is achieved, especially with ARMA graph filters. This confirms our findings in Theorem 2, which means that with a decreasing quantization stepsize, there is no need to perform a robust ARMA filter design since the proposed strategy achieves the optimal steady-state solution.

VII. Conclusion

In this work, we provided a broader analysis of the quantization effects of both FIR and ARMA graph filters over time-invariant and time-varying graphs. We analyzed the impact of fixed and dynamic quantization stepsize on the filtering performance. For FIR filters, we first showed that a dynamic quantization stepsize leads to a more reduction of the quantization MSE than in fixed-stepsize quantization and then we proposed a robust filter design that minimizes the quantization noise. For ARMA graph filters, we showed that decreasing the quantization stepsize over iterations reduces the quantization MSE to zero at steady-state. We extended our quantization effects analysis of FIR and ARMA graph filters to networks affected by random topological changes due to link losses and propose a novel filter design strategy that is robust to quantization and topological changes. Extensive numerical experiments with synthetic and real data show the different trade-offs between quantization bits, filter order, and robustness to topological randomness, ultimately, highlighting the efficiency of the proposed solutions.

As our work puts a new practical paradigm for distributed aspects of graph filters, we identify as relevant future research direction the application of these filters for digital and distributable graph neural networks, network coding, and finite-time consensus.

VIII. Appendix

A. Quantized FIR graph filter output

Considering $\mathbf{x}^{(0)} = \mathbf{x}$ and the quantized message at iterate k, $\tilde{\mathbf{x}}^{(k)} = \mathbf{x}^{(k)} + \mathbf{n}_{\mathrm{q}}^{(k)}$, the output of the shifted graph signal with quantization is:

$$\begin{aligned}
\mathbf{x}^{(1)} &= \mathbf{S}\tilde{\mathbf{x}}^{(0)} = \mathbf{S}(\mathbf{x}^{(0)}+\mathbf{n}_{\mathrm{q}}^{(0)}) = \mathbf{S}\mathbf{x}^{(0)}+\mathbf{S}\mathbf{n}_{\mathrm{q}}^{(0)} \\
\mathbf{x}^{(2)} &= \mathbf{S}\tilde{\mathbf{x}}^{(1)} = \mathbf{S}^2\mathbf{x}^{(0)}+\mathbf{S}^2\mathbf{n}_{\mathrm{q}}^{(0)}+\mathbf{S}\mathbf{n}_{\mathrm{q}}^{(1)} \\
&\vdots \\
\mathbf{x}^{(k)} &= \mathbf{S}^k\,\mathbf{x}^{(0)} + \sum_{\kappa=0}^{k-1}\mathbf{S}^{k-\kappa}\,\mathbf{n}_{\mathrm{q}}^{(\kappa)}, \quad k \geq 1. \qquad (45)
\end{aligned}$$

From (45), the FIR graph filter output with quantization is:

$$\begin{aligned}
\mathbf{y}_{\mathrm{q}} &= \phi_0\mathbf{x} + \phi_1(\mathbf{S}\mathbf{x} + \mathbf{S}\mathbf{n}_{\mathrm{q}}^{(0)}) + \phi_2(\mathbf{S}^2\mathbf{x} + \mathbf{S}^2\mathbf{n}_{\mathrm{q}}^{(0)} + \mathbf{S}\mathbf{n}_{\mathrm{q}}^{(1)}) + \cdots \\
&+ \phi_k(\mathbf{S}^K\mathbf{x} + \mathbf{S}^K\mathbf{n}_{\mathrm{q}}^{(0)} + \mathbf{S}^{K-1}\mathbf{n}_{\mathrm{q}}^{(1)} + \cdots + \mathbf{S}^2\mathbf{n}_{\mathrm{q}}^{(K-2)} + \mathbf{S}\mathbf{n}_{\mathrm{q}}^{(K-1)}) \\
&= \sum_{k=0}^{K}\phi_k\mathbf{S}^k\mathbf{x} + \sum_{k=1}^{K}\phi_k\sum_{\kappa=0}^{k-1}\mathbf{S}^{k-\kappa}\mathbf{n}_{\mathrm{q}}^{(\kappa)}. \qquad (46)
\end{aligned}$$

B. Proof of Proposition 1

By applying the GFT on both sides of (11), the quantization error has the spectral response:

$$\hat{\boldsymbol{\epsilon}} = \sum_{k=1}^{K}\phi_k\sum_{\kappa=0}^{k-1}\boldsymbol{\Lambda}^{k-\kappa}\hat{\mathbf{n}}_{\mathrm{q}}^{(\kappa)} \qquad (47)$$

where $\hat{\mathbf{n}}_{\mathrm{q}}^{(\kappa)}$ is still i.i.d. with same statistics as $\mathbf{n}_{\mathrm{q}}^{(\kappa)}$ iff $\boldsymbol{\Sigma}_{\mathrm{q}\kappa} = \sigma_{\mathrm{q}\kappa}^2\,\mathbf{I}$. From the linearity of the expectation and from the matrix property $(\mathbf{AB})^{\mathrm{H}} = \mathbf{B}^{\mathrm{H}}\mathbf{A}^{\mathrm{H}}$, the quantization noise covariance matrix becomes:

$$\mathbb{E}[\hat{\boldsymbol{\epsilon}}\hat{\boldsymbol{\epsilon}}^{\mathrm{H}}] = \sum_{k_1,k_2=1}^{K}\phi_{k_1}\phi_{k_2}\sum_{\kappa_1=0}^{k_1-1}\sum_{\kappa_2=0}^{k_2-1}\boldsymbol{\Lambda}^{k_1-\kappa_1}\mathbb{E}\Big[\hat{\mathbf{n}}_{\mathrm{q}}^{(\kappa_1)}(\hat{\mathbf{n}}_{\mathrm{q}}^{(\kappa_2)})^{\mathrm{H}}\Big](\boldsymbol{\Lambda}^{k_2-\kappa_2})^{\mathrm{H}}. \qquad (48)$$

Given the quantization noise has independent realizations and a constant quantization stepsize Δ for all iterations, we can rewrite (48) as:

$$\mathbb{E}[\hat{\boldsymbol{\epsilon}}\hat{\boldsymbol{\epsilon}}^{\mathrm{H}}] = \sum_{k=1}^{K}\phi_k^2\sum_{\kappa=0}^{k-1}\boldsymbol{\Lambda}^{k-\kappa}\boldsymbol{\Sigma}_{\mathrm{q}\kappa}(\boldsymbol{\Lambda}^{k-\kappa})^{\mathrm{H}} = \sigma_{\mathrm{q}}^2\sum_{k=1}^{K}\phi_k^2\sum_{\kappa=0}^{k-1}\boldsymbol{\Lambda}^{k-\kappa}(\boldsymbol{\Lambda}^{k-\kappa})^{\mathrm{H}}. \qquad (49)$$

Then, by substituting (49) into the MSE expression $\hat{\zeta}_{\mathrm{q}} = \frac{1}{N}\mathrm{tr}(\mathbb{E}[\hat{\boldsymbol{\epsilon}}\hat{\boldsymbol{\epsilon}}^{H}])$ and using the relation between the Frobenius norm and the trace $\|\mathbf{A}\|_F = \sqrt{\mathrm{tr}(\mathbf{A}\mathbf{A}^{H})}$, result (12) yields.

C. Proof of Corollary 1.1

From (12) and the relation between the l_2-norm and the Frobenius norm $\|\mathbf{A}\|_F \leq \sqrt{r}\|\mathbf{A}\|_2$ with r the rank of $\mathbf{A}$ (at most N), $\hat{\zeta}_{\mathrm{q}}$ can be upper bounded as:

$$\hat{\zeta}_{\mathrm{q}} \leq N\frac{\sigma_{\mathrm{q}}^2}{N}\sum_{k=1}^{K}\phi_k^2\sum_{\kappa=0}^{k-1}\|\boldsymbol{\Lambda}^{k-\kappa}\|_2^2 \leq \sigma_{\mathrm{q}}^2\sum_{k=1}^{K}\phi_k^2\sum_{\kappa=0}^{k-1}(\lambda_{\max}^2)^{k-\kappa}. \qquad (50)$$

Similarly, by exploiting again the relationship between the l_2-norm and Frobenius norm of matrices ($\|\mathbf{A}\|_2 \leq \|\mathbf{A}\|_F$) in (12), $\hat{\zeta}_{\mathrm{q}}$ can be likewise lower bounded as:

$$\hat{\zeta}_{\mathrm{q}} \geq \frac{\sigma_{\mathrm{q}}^2}{N}\sum_{k=1}^{K}\phi_k^2\sum_{\kappa=0}^{k-1}(\lambda_{\max}^2)^{k-\kappa} \qquad (51)$$

where (50) and (51) bound the quantization MSE. If $\lambda_{\max} \neq 1$ and making the index change $\sum_{\tau=0}^{k-1}a^{k-\tau} = \sum_{\tau=1}^{k}a^{\tau}$, we obtain the finite geometric series whose argument is different from one; thus, $\hat{\zeta}_{\mathrm{q}}$ can be lower and upper bound as in (13).

D. Proof of Proposition 2

By equivalence to (12), the MSE on the filter output due to the quantization noise has the form:

$$\hat{\zeta}_{\mathrm{q}} = \frac{1}{N}\sum_{k=1}^{K}\phi_k^2\sum_{\kappa=0}^{k-1}\sigma_{\mathrm{q}\kappa}^2\|\boldsymbol{\Lambda}^{k-\kappa}\|_F^2 \leq \sum_{k=1}^{K}\phi_k^2\sum_{\kappa=0}^{k-1}\sigma_{\mathrm{q}\kappa}^2(\lambda_{\max}^2)^{k-\kappa}. \qquad (52)$$

To decrease the MSE, we choose, for the convenience of the proof, the stepsize $\Delta_\kappa = (\lambda_{\max})^{\kappa}\Delta_0$, which implies:

$$\hat{\zeta}_{\mathrm{q}} \leq \frac{\Delta_0^2}{12}\sum_{k=1}^{K}\phi_k^2\;k\;\lambda_{\max}^{2k}. \qquad (53)$$

Under the assumption $0 \leq \lambda_{\max} \leq 1$ in (53), we can write:

$$\hat{\zeta}_{\mathrm{q}} \leq \frac{\Delta_0^2}{12}\sum_{k=1}^{K}\phi_k^2\;k \qquad (54)$$

where the final bound can be written as (14).

E. Proof of Proposition 3

By using (20c), the trace cyclic property $\mathrm{tr}(\mathbf{ABC}) = \mathrm{tr}(\mathbf{CAB})$, the inequality $\mathrm{tr}(\mathbf{AB}) \leq \|\mathbf{A}\|_2\mathrm{tr}(\mathbf{B})$ –which holds for any positive semi-definite matrix $\mathbf{B} \succeq \mathbf{0}$ and square matrix

$\mathbf{A}$ of appropriate dimensions [60]–, and the linearity of the expectation w.r.t the trace, we can write:

$$\begin{aligned}\zeta_{yt}^{\mathrm{q}} &= \frac{1}{N}\mathbb{E}[\mathrm{tr}((\mathbf{1}^\top \otimes \mathbf{I}_N)^{\mathrm{H}})(\mathbf{1}^\top \otimes \mathbf{I}_N)\boldsymbol{\epsilon}_t^{\mathrm{q}}(\boldsymbol{\epsilon}_t^{\mathrm{q}})^{\mathrm{H}}] \\ &\leq \frac{1}{N}\|(\mathbf{1}^\top \otimes \mathbf{I}_N)^{\mathrm{H}}(\mathbf{1}^\top \otimes \mathbf{I}_N)\|_2 \ \mathrm{tr}(\mathbb{E}[\boldsymbol{\epsilon}_t^{\mathrm{q}}(\boldsymbol{\epsilon}_t^{\mathrm{q}})^{\mathrm{H}}]).\end{aligned} \tag{55}$$

Then, by substituting $\boldsymbol{\epsilon}_t^{\mathrm{q}} = \sum_{\tau=0}^{t-1}(\boldsymbol{\Psi} \otimes \mathbf{S})^{t-\tau}\mathbf{n}_\tau^{\mathrm{q}}$ in (55), $\mathbb{E}[\mathbf{n}_\tau^{\mathrm{q}}(\mathbf{n}_\tau^{\mathrm{q}})^{\mathrm{H}}] = \sigma_{\mathrm{q}}^2\mathbf{I}$ which holds for fixed quantization stepsize in each iteration, and since $\|(\mathbf{1}^\top \otimes \mathbf{I}_N)^{\mathrm{H}}(\mathbf{1}^\top \otimes \mathbf{I}_N)\|_2 = K$, we can write:

$$\zeta_{yt}^{\mathrm{q}} \leq \frac{K\sigma_{\mathrm{q}}^2}{N}\sum_{\tau=0}^{t-1}\mathrm{tr}\left((\boldsymbol{\Psi} \otimes \mathbf{S})^{t-\tau}((\boldsymbol{\Psi} \otimes \mathbf{S})^{t-\tau})^{\mathrm{H}}\right). \tag{56}$$

By using in (56) the index change $\sum_{\tau=0}^{t-1}\mathbf{A}^{t-\tau}(\mathbf{A}^{t-\tau})^{\mathrm{H}} = \sum_{\tau=1}^{t}\mathbf{A}^{\tau}(\mathbf{A}^{\tau})^{\mathrm{H}}$, the Frobenius norm $\|\mathbf{A}\|_F = \sqrt{\mathrm{tr}(\mathbf{A}\mathbf{A}^{\mathrm{H}})}$, the inequality $\|\mathbf{A}\|_F \leq \sqrt{r}\|\mathbf{A}\|_2$, with r the rank of $\mathbf{A}$ (at most N), and the triangle inequality of the norms $\|\mathbf{A}^2\|_2 \leq \|\mathbf{A}\|_2^2$, we have:

$$\zeta_{yt}^{\mathrm{q}} \leq \frac{K\sigma_{\mathrm{q}}^2}{N}\sum_{\tau=1}^{t}\|(\boldsymbol{\Psi} \otimes \mathbf{S})^{\tau}\|_F^2 \leq K\sigma_{\mathrm{q}}^2\sum_{\tau=1}^{t}\|(\boldsymbol{\Psi} \otimes \mathbf{S})\|_2^{2\tau}. \tag{57}$$

Then, from the Kronecker product identity $\|\mathbf{A} \otimes \mathbf{B}\|_2 = \|\mathbf{A}\|_2\|\mathbf{B}\|_2$ and the l_2-norm matrix norm expression $\|\mathbf{A}\|_2 = \sqrt{\max\mathrm{eig}(\mathbf{A}^{\mathrm{H}}\mathbf{A})}$, we can further rewrite (57) as:

$$\zeta_{yt}^{\mathrm{q}} \leq K\sigma_{\mathrm{q}}^2\sum_{\tau=1}^{t}\|\boldsymbol{\Psi}\|_2^{2\tau}\|\mathbf{S}\|_2^{2\tau} \leq K\sigma_{\mathrm{q}}^2\sum_{\tau=1}^{t}(\psi_{\max}\lambda_{\max})^{2\tau}. \tag{58}$$

Finally, since (58) is a finite geometric series with an argument smaller than one, the quantization MSE ζ_{yt}^{q} can be upper bounded by (21).

F. Proof of Theorem 1

By equivalence to (56), but with a dynamic quantization stepsize, the MSE on the filter output due to the quantization noise is upper bounded by:

$$\begin{aligned}\zeta_{yt}^{\mathrm{q}} &\leq \frac{K}{N}\sum_{\tau=0}^{t-1}\sigma_{\mathrm{q}\tau}^2\mathrm{tr}((\boldsymbol{\Psi} \otimes \mathbf{S})^{t-\tau}((\boldsymbol{\Psi} \otimes \mathbf{S})^{t-\tau})^{\mathrm{H}}) \\ &\leq \frac{K}{12N}\sum_{\tau=1}^{t}\Delta_{t-\tau}^2\|(\boldsymbol{\Psi} \otimes \mathbf{S})^{\tau}\|_F^2 \leq \frac{K}{12}\sum_{\tau=1}^{t}\Delta_{t-\tau}^2(\psi_{\max}\lambda_{\max})^{2\tau}\end{aligned} \tag{59}$$

where similarily to (57) and (58), we changed the summatiom index, used the expression of the Frobenius norm $\|\mathbf{A}\|_F = \sqrt{\mathrm{tr}(\mathbf{A}\mathbf{A}^{\mathrm{H}})}$, and leveraged the norm properties.

For the quantization stepsize $\Delta_\tau = (\psi_{\max}\lambda_{\max})^{\tau}\Delta_0$, (59) can be further upper bounded as:

$$\zeta_{yt}^{\mathrm{q}} \leq \frac{K}{12}\sum_{\tau=1}^{t}(\psi_{\max}\lambda_{\max})^{2t}\Delta_0 \tag{60}$$

which can be easily rephrased as in (24).

G. Quantized FIR graph filter over time-varying graphs

Considering $\mathbf{x}^{(0)} = \mathbf{x}$ and the quantized message at iterate k, $\tilde{\mathbf{x}}^{(k)} = \mathbf{x}^{(k)} + \mathbf{n}_{\mathrm{q}}^{(k)}$, the output of the shifted graph signal with quantization performed over $\mathcal{G}_t$ is:

$$\begin{aligned}\mathbf{x}^{(1)} &= \mathbf{S}_{t-1}\tilde{\mathbf{x}}^{(0)} = \mathbf{S}_{t-1}(\mathbf{x}^{(0)}+\mathbf{n}_{\mathrm{q}}^{(0)}) = \mathbf{S}_{t-1}\mathbf{x}^{(0)}+\mathbf{S}_{t-1}\mathbf{n}_{\mathrm{q}}^{(0)} \\ \mathbf{x}^{(2)} &= \mathbf{S}_{t-2}\tilde{\mathbf{x}}^{(1)} = \mathbf{S}_{t-2}\mathbf{S}_{t-1}\mathbf{x}^{(0)}+\mathbf{S}_{t-2}\mathbf{S}_{t-1}\mathbf{n}_{\mathrm{q}}^{(0)}+\mathbf{S}_{t-2}\mathbf{n}_{\mathrm{q}}^{(1)} \\ &\vdots \\ \mathbf{x}^{(k)} &= \left(\prod_{\tau=t-1}^{t-k}\mathbf{S}_\tau\right)\mathbf{x}^{(0)} + \sum_{\kappa=0}^{k-1}\left(\prod_{\tau=t-1-\kappa}^{t-k}\mathbf{S}_\tau\right)\mathbf{n}_{\mathrm{q}}^{(\kappa)}, \ \ k \geq 1.\end{aligned} \tag{61}$$

The quantized output of FIR graph filter at iteration t, performed over $\mathcal{G}_t$ with quantization effects, is given by:

$$\begin{aligned}\mathbf{y}_t^{\mathrm{q}} &= \phi_0\,\mathbf{x} + \sum_{k=1}^{K}\phi_k\,\mathbf{x}^{(k)} \\ &= \phi_0\,\mathbf{x} + \sum_{k=1}^{K}\phi_k\left(\boldsymbol{\Theta}(t-1,t-k)\,\mathbf{x}^{(0)} + \sum_{\kappa=0}^{k-1}\boldsymbol{\Theta}(t-1-\kappa,t-k)\,\mathbf{n}_{\mathrm{q}}^{(\kappa)}\right) \\ &= \sum_{k=0}^{K}\phi_k\boldsymbol{\Theta}(t-1,t-k)\mathbf{x} + \sum_{k=1}^{K}\sum_{\kappa=0}^{k-1}\phi_k\,\boldsymbol{\Theta}(t-1-\kappa,t-k)\,\mathbf{n}_{\mathrm{q}}^{(\kappa)}.\end{aligned} \tag{62}$$

H. Proof of Proposition 4

By using $\|\mathbf{x}\|_2^2 = \mathrm{tr}(\mathbf{x}\mathbf{x}^{\mathrm{H}})$ and rearranging the summation indices, we can write the MSE of the filter output due quantization and graph randomness as:

$$\begin{aligned}\zeta_t^{\mathrm{q}} &= \mathbb{E}[\frac{1}{N}\mathrm{tr}(\boldsymbol{\epsilon}_t{\boldsymbol{\epsilon}_t}^H)] = \frac{1}{N}\mathbb{E}[\|\boldsymbol{\epsilon}_t\|_2^2] \\ &= \frac{1}{N}\mathbb{E}\left[\left\|\sum_{\kappa=1}^{K}\sum_{k=\kappa}^{K}\phi_k\,\boldsymbol{\Theta}(t-\kappa,t-k)\,\mathbf{n}_{\mathrm{q}}^{(\kappa-1)}\right\|_2^2\right].\end{aligned} \tag{63}$$

Let then vector $\boldsymbol{\omega}(\kappa,t) = \sum_{k=\kappa}^{K}\phi_k\boldsymbol{\Theta}(t-\kappa,t-k)\ \ \mathbf{n}_{\mathrm{q}}^{(\kappa-1)}$ account for the accumulated quantization noise over time-varying graphs. By using $\|\mathbf{x}\|_2^2 = \mathbf{x}^{\mathrm{H}}\mathbf{x}$, we can write:

$$\mathbb{E}\left[\left\|\sum_{\kappa=1}^{K}\boldsymbol{\omega}(\kappa,t)\right\|_2^2\right] = \sum_{\kappa_1=1}^{K}\sum_{\kappa_2=1}^{K}\mathbb{E}\Big[\boldsymbol{\omega}(\kappa_1,t)^{\mathrm{H}}\boldsymbol{\omega}(\kappa_2,t)\Big]. \tag{64}$$

Since the quantization errors are zero mean and independent from graph topology processes, we have:

$$\mathbb{E}\Big[\boldsymbol{\omega}(\kappa_1,t)^{\mathrm{H}}\boldsymbol{\omega}(\kappa_2,t)\Big] = \begin{cases} 0 & \text{if } \kappa_1 \neq \kappa_2 \\ \mathbb{E}[\|\boldsymbol{\omega}(\kappa_1,t)\|_2^2] & \text{if } \kappa_1 = \kappa_2. \end{cases} \tag{65}$$

Therefore, we can rewrite (65) as:

$$\mathbb{E}\left[\left\|\sum_{\kappa=1}^{K}\boldsymbol{\omega}(\kappa,t)\right\|_2^2\right] = \sum_{\kappa=1}^{K}\mathbb{E}\Big[\big\|\boldsymbol{\omega}(\kappa,t)\big\|_2^2\Big]. \tag{66}$$

Using once again the norm property $\|\mathbf{x}\|_2^2 = \mathrm{tr}(\mathbf{x}\mathbf{x}^{\mathrm{H}})$, the cyclic property of the trace $\mathrm{tr}(\mathbf{ABC}) = \mathrm{tr}(\mathbf{CAB})$, and the commutativity of the trace to respect to the expectation, we can write:

$$\begin{aligned}\mathbb{E}[\|\boldsymbol{\epsilon}_t\|_2^2] &= \sum_{\kappa=1}^{K}\mathbb{E}\Big[\mathrm{tr}\Big(\Big(\sum_{k=\kappa}^{K}\phi_k\boldsymbol{\Theta}(t-\kappa,t-k)\Big)\,\mathbf{n}_{\mathrm{q}}^{(\kappa-1)}(\mathbf{n}_{\mathrm{q}}^{(\kappa-1)})^{\mathrm{H}} \\ &\qquad \times\Big(\sum_{k=\kappa}^{K}\phi_k\boldsymbol{\Theta}(t-\kappa,t-k)\Big)^{\mathrm{H}}\Big)\Big] \\ &= \sum_{\kappa=1}^{K}\mathrm{tr}\Big(\mathbb{E}\Big[\Big(\sum_{k=\kappa}^{K}\phi_k\boldsymbol{\Theta}(t-\kappa,t-k)^{\mathrm{H}}\Big)\Big(\sum_{k=\kappa}^{K}\phi_k\boldsymbol{\Theta}(t-\kappa,t-k)\Big)\Big] \\ &\qquad \times\mathbb{E}\big[\mathbf{n}_{\mathrm{q}}^{(\kappa-1)}(\mathbf{n}_{\mathrm{q}}^{(\kappa-1)})^{\mathrm{H}}\big]\Big).\end{aligned} \tag{67}$$

By using the inequality $\mathrm{tr}(\mathbf{AB}) \leq \|\mathbf{A}\|_2\,\mathrm{tr}(\mathbf{B})$, we obtain:

$$\begin{aligned}\mathbb{E}[\|\boldsymbol{\epsilon}_t\|_2^2] &\leq \sum_{\kappa=1}^{K}\mathrm{tr}\Big(\mathbb{E}\big[\mathbf{n}_{\mathrm{q}}^{(\kappa-1)}(\mathbf{n}_{\mathrm{q}}^{(\kappa-1)})^{\mathrm{H}}\big]\Big) \\ &\times\left\|\mathbb{E}\Big[\Big(\sum_{k=\kappa}^{K}\phi_k\boldsymbol{\Theta}(t-\kappa,t-k)^{\mathrm{H}}\Big)\Big(\sum_{k=\kappa}^{K}\phi_k\boldsymbol{\Theta}(t-\kappa,t-k)\Big)\Big]\right\|_2.\end{aligned} \tag{68}$$

Since $\mathrm{tr}\big(\mathbb{E}\big[\mathbf{n}_{\mathrm{q}}^{(\kappa)}(\mathbf{n}_{\mathrm{q}}^{(\kappa)})^{\mathrm{H}}\big]\big) = \mathrm{tr}\big(\sigma_{\mathrm{q}\kappa}^2\mathbf{I}\big) = N\sigma_{\mathrm{q}\kappa}^2$ and using the Jensen's inequality of the spectral norm ($\|\mathbb{E}[\mathbf{A}]\|_2 \leq \mathbb{E}[\|\mathbf{A}\|_2]$), we can further write:

$$\begin{aligned}&\mathbb{E}[\|\boldsymbol{\epsilon}_t\|_2^2] \leq \\ &N\sum_{\kappa=1}^{K}\sigma_{\mathrm{q}\kappa-1}^2\mathbb{E}\bigg[\bigg\|\Big(\sum_{k=\kappa}^{K}\phi_k\boldsymbol{\Theta}(t-\kappa,t-k)^{\mathrm{H}}\Big)\Big(\sum_{k=\kappa}^{K}\phi_k\boldsymbol{\Theta}(t-\kappa,t-k)\Big)\bigg\|_2\bigg] \\ &\leq \frac{N}{12}\sum_{\kappa=1}^{K}\Delta_{\kappa-1}^2\,\mathbb{E}\big[\Upsilon(t,\kappa)\big]\end{aligned} \tag{69}$$

where $\Upsilon(t,\kappa)$ is:

$$\Upsilon(t,\kappa) = \bigg\|\Big(\sum_{k=\kappa}^{K}\phi_k\boldsymbol{\Theta}(t-\kappa,t-k)^{\mathrm{H}}\Big)\Big(\sum_{k=\kappa}^{K}\phi_k\boldsymbol{\Theta}(t-\kappa,t-k)\Big)\bigg\|_2. \tag{70}$$

By using the spectral norm sub-multiplicativity $\|\mathbf{AB}\|_2 \leq \|\mathbf{A}\|_2\|\mathbf{B}\|_2$ and subadditivity $\|\mathbf{A}+\mathbf{B}\|_2 \leq \|\mathbf{A}\|_2+\|\mathbf{B}\|_2$ along with the upper bound of the shift operator $\|\mathbf{S}_t\|_2 \leq \|\mathbf{S}\|_2 \leq \rho$ for all t, we upper bound (70) as:

$$\begin{aligned}\Upsilon(t,\kappa) &\leq \bigg\|\sum_{k=\kappa}^{K}\phi_k\boldsymbol{\Theta}(t-\kappa,t-k)^{\mathrm{H}}\bigg\|_2\,\bigg\|\sum_{k=\kappa}^{K}\phi_k\boldsymbol{\Theta}(t-\kappa,t-k)\bigg\|_2 \\ &\leq \bigg(\sum_{k=\kappa}^{K}\rho^{k-\kappa+1}\,|\phi_k|\bigg)^2.\end{aligned} \tag{71}$$

Finally, by substituting (71) into (69) and computing the expectation, ζ_t^{q} can be upper bounded by (29).

I. Proof of Theorem 2

Similarly to (55), we can write the MSE of ARMA filter due to quantization and graph randomness (38c) as:

$$\xi_{yt}^{\mathrm{q}} \leq \frac{1}{N}\|(\mathbf{1}^\top\otimes\mathbf{I}_N)^{\mathrm{H}}(\mathbf{1}^\top\otimes\mathbf{I}_N)\|_2\mathrm{tr}(\mathbb{E}[\boldsymbol{\varepsilon}_t^{\mathrm{q}}(\boldsymbol{\varepsilon}_t^{\mathrm{q}})^{\mathrm{H}}]) \leq \frac{K}{N}\mathrm{tr}(\mathbb{E}[\boldsymbol{\varepsilon}_t^{\mathrm{q}}(\boldsymbol{\varepsilon}_t^{\mathrm{q}})^{\mathrm{H}}]). \tag{72}$$

Then, by substituting $\boldsymbol{\varepsilon}_t^{\mathrm{q}}$ with its expression, using the linearity of the expectation w.r.t the trace, the cyclic property of the trace $\mathrm{tr}(\mathbf{ABC}) = \mathrm{tr}(\mathbf{CAB})$, we can write:

$$\begin{aligned}\mathrm{tr}(\mathbb{E}[\boldsymbol{\varepsilon}_t^{\mathrm{q}}(\boldsymbol{\varepsilon}_t^{\mathrm{q}})^{\mathrm{H}}]) &= \sum_{\tau_1=0}^{t-1}\sum_{\tau_2=0}^{t-1}\mathbb{E}\bigg[\mathrm{tr}\Big(\Big(\prod_{\varsigma=\tau_2}^{t-1}\boldsymbol{\Psi}\otimes\mathbf{S}_\varsigma\Big)^{\mathrm{H}} \\ &\times\Big(\prod_{\varsigma=\tau_1}^{t-1}\boldsymbol{\Psi}\otimes\mathbf{S}_\varsigma\Big)\,\mathbf{n}_{\tau_1}^{\mathrm{q}}(\mathbf{n}_{\tau_2}^{\mathrm{q}})^{\mathrm{H}}\Big)\bigg] \\ &= \sum_{\tau_1=0}^{t-1}\sum_{\tau_2=0}^{t-1}\mathrm{tr}\Big(\mathbb{E}\Big[\Big(\prod_{\varsigma=\tau_2}^{t-1}\boldsymbol{\Psi}\otimes\mathbf{S}_\varsigma\Big)^{\mathrm{H}}\Big(\prod_{\varsigma=\tau_1}^{t-1}\boldsymbol{\Psi}\otimes\mathbf{S}_\varsigma\Big)\Big] \\ &\times\mathbb{E}[\mathbf{n}_{\tau_1}^{\mathrm{q}}(\mathbf{n}_{\tau_2}^{\mathrm{q}})^{\mathrm{H}}]\Big).\end{aligned} \tag{73}$$

By considering $\mathbb{E}[\mathbf{n}_{\tau_1}^{\mathrm{q}}(\mathbf{n}_{\tau_2}^{\mathrm{q}})^{\mathrm{H}}] = \mathbf{0}$ if $\tau_1 \neq \tau_2$, using the inequality $\mathrm{tr}(\mathbf{AB}) \leq \|\mathbf{A}\|_2\,\mathrm{tr}(\mathbf{B})$, assuming unified quantization with dynamic stepsize i.e., $\mathrm{tr}(\mathbb{E}[\mathbf{n}_\tau^{\mathrm{q}}(\mathbf{n}_\tau^{\mathrm{q}})^{\mathrm{H}}]) = KN\sigma_{\mathrm{q},\tau}^2$ and using the Jensen's inequality of the spectral norm ($\|\mathbb{E}[\mathbf{A}]\|_2 \leq \mathbb{E}[\|\mathbf{A}\|_2]$), we can write:

$$\mathrm{tr}(\mathbb{E}[\boldsymbol{\varepsilon}_t^{\mathrm{q}}(\boldsymbol{\varepsilon}_t^{\mathrm{q}})^{\mathrm{H}}]) \leq KN\sum_{\tau=0}^{t-1}\sigma_{\mathrm{q},\tau}^2\mathbb{E}\bigg[\bigg\|\Big(\prod_{\varsigma=\tau}^{t-1}\boldsymbol{\Psi}\otimes\mathbf{S}_\varsigma\Big)^{\mathrm{H}}\Big(\prod_{\varsigma=\tau}^{t-1}\boldsymbol{\Psi}\otimes\mathbf{S}_\varsigma\Big)\bigg\|_2\bigg]. \tag{74}$$

By using the sub-multiplicativity property of the spectral norm of a square matrix i.e., $\|\mathbf{AB}\|_2 \leq \|\mathbf{A}\|_2\|\mathbf{B}\|_2$, the property $\|\mathbf{A}\otimes\mathbf{B}\|_2 = \|\mathbf{A}\|_2\|\mathbf{B}\|_2$ and assuming that the spectral norm of the shift operator used is upper bounded i.e., $\|\mathbf{S}\|_2 \leq \|\mathbf{S}_t\|_2 \leq \rho$ for all t, we have:

$$\begin{aligned}\bigg\|\Big(\prod_{\varsigma=\tau}^{t-1}\boldsymbol{\Psi}\otimes\mathbf{S}_\varsigma\Big)^{\mathrm{H}}\Big(\prod_{\varsigma=\tau}^{t-1}\boldsymbol{\Psi}\otimes\mathbf{S}_\varsigma\Big)\bigg\|_2 &\leq \Big(\prod_{\varsigma=\tau}^{t-1}\|\boldsymbol{\Psi}\|_2\|\mathbf{S}_\varsigma\|_2\Big)\Big(\prod_{\varsigma=\tau}^{t-1}\|\boldsymbol{\Psi}\|_2\|\mathbf{S}_\varsigma\|_2\Big). \\ &\leq (\psi_{\max}\,\rho)^{2t-2\tau}.\end{aligned} \tag{75}$$

By applying the expectation to (75) and combining it with (74) and (72), and making an index change using $\sum_{\tau=0}^{t-1}c_\tau a^{t-\tau} = \sum_{\tau=1}^{t}c_{t-\tau}a^\tau$, we can write:

$$\begin{aligned}\xi_{yt}^{\mathrm{q}} &\leq K^2\sum_{\tau=0}^{t-1}\sigma_{\mathrm{q},\tau}^2\big((\psi_{\max}\,\rho)^2\big)^{t-\tau} \leq K^2\sum_{\tau=1}^{t}\sigma_{\mathrm{q},t-\tau}^2\big((\psi_{\max}\,\rho)^2\big)^{\tau} \\ &\leq \frac{K^2}{12}\sum_{\tau=1}^{t}\Delta_{t-\tau}^2(\psi_{\max}\,\rho)^{2\tau}.\end{aligned} \tag{76}$$

With the choice of the quantization stepsize $\Delta_\tau = (\psi_{\max}\,\rho)^\tau\Delta_0$, the final bound in (76) becomes:

$$\xi_{yt}^{\mathrm{q}} \leq \frac{K^2}{12}\sum_{\tau=1}^{t}(\psi_{\max}\,\rho)^{2t}\Delta_0. \tag{77}$$

Therefore, ξ_{yt}^{q} can be upper bounded by (39).

REFERENCES

[1] L. Ben Saad, E. Isufi, and B. Beferull-Lozano, "Graph filtering with quantization over random time-varying graphs," in *IEEE Global Conference on Signal and Information Processing*, Nov 2019, pp. 1–5.

[2] D. I. Shuman, S. K. Narang, P. Frossard, A. Ortega, and P. Vandergheynst, "The emerging field of signal processing on graphs: Extending high-dimensional data analysis to networks and other irregular domains," *IEEE Sig. Process. Mag.*, vol. 30, no. 3, pp. 83–98, May 2013.

[3] F. Gama, E. Isufi, G. Leus, and A. Ribeiro, "Graphs, convolutions, and neural networks," *arXiv preprint arXiv:2003.03777*, Mar 2020.

[4] W. Huang, L. Goldsberry, N. F. Wymbs, S. T. Grafton, D. S. Bassett, and A. Ribeiro, "Graph frequency analysis of brain signals," *IEEE J. Sel. Topics Sig. Process.*, vol. 10, no. 7, pp. 1189–1203, 2016.

[5] D. B. Burkhardt, J. S. Stanley, A. L. Perdigoto, S. A. Gigante, K. C. Herold, G. Wolf, A. Giraldez, D. van Dijk, and S. Krishnaswamy, "Enhancing experimental signals in single-cell RNA-sequencing data using graph signal processing," *bioRxiv*, 2019.

[6] W. Huang, A. G. Marques, and A. R. Ribeiro, "Rating prediction via graph signal processing," *IEEE Transactions on Signal Processing*, vol. 66, no. 19, pp. 5066–5081, 2018.

[7] A. Sandryhaila and J. M. Moura, "Discrete signal processing on graphs: Frequency analysis," *IEEE Trans. Signal Processing*, vol. 62, no. 12, pp. 3042–3054, 2014.

[8] B. Girault, P. Gonçalves, E. Fleury, and A. S. Mor, "Semi-supervised learning for graph to signal mapping: A graph signal wiener filter interpretation," in *Proc. IEEE Int. Conf. Acoust., Speech, Sig. Process.* IEEE, 2014, pp. 1115–1119.

[9] N. Tremblay, G. Puy, R. Gribonval, and P. Vandergheynst, "Compressive spectral clustering," in *International Conference on Machine Learning*, 2016, pp. 1002–1011.

[10] A. Loukas, M. Zuniga, I. Protonotarios, and J. Gao, "How to identify global trends from local decisions? event region detection on mobile networks," in *IEEE INFOCOM*, 2014, pp. 1177–1185.

[11] E. Isufi, A. Loukas, A. Simonetto, and G. Leus, "Autoregressive moving average graph filtering," *IEEE Trans. Sig. Process.*, vol. 65, no. 2, pp. 274–288, Jan 2017.

[12] M. Eisen and A. Ribeiro, "Optimal wireless resource allocation with random edge graph neural networks," *arXiv:1909.01865*, Nov 2019.

[13] E. Isufi, A. Loukas, N. Perraudin, and G. Leus, "Forecasting time series with varma recursions on graphs," *IEEE Transactions on Signal Processing*, vol. 67, no. 18, pp. 4870–4885, Sep. 2019.

[14] L. Ben Saad and B. Beferull-Lozano, "Accurate graph filtering in wireless sensor networks," *IEEE Internet of Things Journal*, vol. 7, no. 12, pp. 11 431–11 445, 2020.

[15] R. Nassif, C. Richard, J. Chen, and A. H. Sayed, "Distributed diffusion adaptation over graph signals," in *Proc. IEEE Int. Conf. Acoust., Speech, Sig. Process.*, April 2018, pp. 4129–4133.

[16] S. Segarra, A. G. Marques, G. Leus, and A. Ribeiro, "Reconstruction of graph signals through percolation from seeding nodes," *IEEE Transactions on Signal Processing*, vol. 64, no. 16, pp. 4363–4378, 2016.

[17] E. Isufi, P. Di Lorenzo, P. Banelli, and G. Leus, "Distributed wiener-based reconstruction of graph signals," in *2018 IEEE Statistical Signal Processing Workshop (SSP)*, June 2018, pp. 21–25.

[18] D. I. Shuman, P. Vandergheynst, D. Kressner, and P. Frossard, "Distributed signal processing via chebyshev polynomial approximation," *IEEE Trans. Sig. Info. Process. Netw.*, vol. 4, no. 4, pp. 736–751, 2018.

[19] S. Chen, A. Sandryhaila, J. M. F. Moura, and J. Kovacevic, "Signal denoising on graphs via graph filtering," in *Global Conf. Sig. Inf. Process.*, Dec 2014, pp. 872–876.

[20] A. Sandryhaila, S. Kar, and J. M. Moura, "Finite-time distributed consensus through graph filters," in *Proc. IEEE Int. Conf. Acoust., Speech, Sig. Process.* IEEE, 2014, pp. 1080–1084.

[21] E. Tolstaya, F. Gama, J. Paulos, G. Pappas, V. Kumar, and A. Ribeiro, "Learning decentralized controllers for robot swarms with graph neural networks," *arXiv preprint arXiv:1903.10527*, Sep 2019.

[22] S. Segarra, A. G. Marques, and A. Ribeiro, "Optimal graph-filter design and applications to distributed linear network operators," *IEEE Trans. Sig. Process.*, vol. 65, no. 15, pp. 4117–4131, Aug 2017.

[23] A. Sandryhaila and J. M. Moura, "Discrete signal processing on graphs," *IEEE Trans. Sig. Process.*, vol. 61, no. 7, pp. 1644–1656, 2013.

[24] M. Coutino, E. Isufi, and G. Leus, "Advances in distributed graph filtering," *IEEE Trans. Sig. Process.*, vol. 67, no. 9, pp. 2320–2333, May 2019.

[25] R. Levie, E. Isufi, and G. Kutyniok, "On the transferability of spectral graph filters," in *13th International conference on Sampling Theory and Applications (SampTA)*, 2019, pp. 1–5.

[26] E. Isufi, A. Loukas, A. Simonetto, and G. Leus, "Filtering random graph processes over random time-varying graphs," *IEEE Trans. Sig. Process.*, vol. 65, no. 16, pp. 4406–4421, Aug 2017.

[27] T. C. Aysal, M. Coates, and M. Rabbat, "Distributed average consensus using probabilistic quantization," in *IEEE/SP 14th Workshop on Statistical Signal Processing*, Aug 2007, pp. 640–644.

[28] T. C. Aysal, M. J. Coates, and M. G. Rabbat, "Distributed average consensus with dithered quantization," *IEEE Transactions on Signal Processing*, vol. 56, no. 10, pp. 4905–4918, Oct 2008.

[29] Jun Fang and Hongbin Li, "An adaptive quantization scheme for distributed consensus," in *Proc. IEEE Int. Conf. Acoust., Speech, Sig. Process.*, April 2009, pp. 2777–2780.

[30] R. Carli, F. Fagnani, P. Frasca, and S. Zampieri, "Gossip consensus algorithms via quantized communication," *Automatica*, vol. 46, no. 1, pp. 70 – 80, 2010.

[31] S. Kar and J. M. F. Moura, "Distributed consensus algorithms in sensor networks: Quantized data and random link failures," *IEEE Transactions on Signal Processing*, vol. 58, no. 3, pp. 1383–1400, March 2010.

[32] K. Cai and H. Ishii, "Gossip consensus and averaging algorithms with quantization," in *American Control Conf.*, June 2010, pp. 6306–6311.

[33] D. Thanou, E. Kokiopoulou, Y. Pu, and P. Frossard, "Distributed average consensus with quantization refinement," *IEEE Transactions on Signal Processing*, vol. 61, no. 1, pp. 194–205, Jan 2013.

[34] S. Zhu and B. Chen, "Quantized consensus by the admm: Probabilistic versus deterministic quantizers," *IEEE Transactions on Signal Processing*, vol. 64, no. 7, pp. 1700–1713, April 2016.

[35] L. F. O. Chamon and A. Ribeiro, "Finite-precision effects on graph filters," in *Global Conf. Sig. Inf. Process.*, Nov 2017, pp. 603–607.

[36] I. C. M. Nobre and P. Frossard, "Optimized quantization in distributed graph signal filtering," *arXiv preprint arXiv:1909.12725*, Sep 2019.

[37] D. Thanou and P. Frossard, "Learning of robust spectral graph dictionaries for distributed processing," *EURASIP Journal on Advances in Signal Processing*, vol. 2018, no. 1, p. 67, Oct 2018.

[38] L. Schuchman, "Dither signals and their effect on quantization noise," *IEEE Trans. Commun. Tech.*, vol. 12, no. 4, pp. 162–165, Dec 1964.

[39] S. P Lipshitz, R. Wannamaker, and J. Vanderkooy, "Quantization and dither: A theoretical survey," *Journal of the Audio Engineering Society*, vol. 40, pp. 355–374, 05 1992.

[40] A. G. Marques, S. Segarra, G. Leus, and A. Ribeiro, "Sampling of graph signals with successive local aggregations," *IEEE Trans. Sig. Process.*, vol. 64, no. 7, pp. 1832–1843, 2016.

[41] J. Liu, E. Isufi, and G. Leus, "Filter design for autoregressive moving average graph filters," *IEEE Transactions on Signal and Information Processing over Networks*, vol. 5, no. 1, pp. 47–60, March 2019.

[42] X. Zhan, "Extremal eigenvalues of real symmetric matrices with entries in an interval," *SIAM J. Matrix Anal. Appl.*, vol. 27, pp. 851–860, 2005.

[43] K. C. Das and R. B. Bapat, "A sharp upper bound on the spectral radius of weighted graphs," vol. 308, no. 15, pp. 3180–3186, Aug. 2008.

[44] B. Widrow and I. Kollár, *Quantization Noise: Roundoff Error in Digital Computation, Signal Processing, Control, and Communications*. Cambridge University Press, 2008.

[45] R. M. Gray and D. L. Neuhoff, "Quantization," *IEEE Transactions on Information Theory*, vol. 44, no. 6, pp. 2325–2383, Oct 1998.

[46] A. Sripad and D. Snyder, "A necessary and sufficient condition for quantization errors to be uniform and white," *IEEE Trans. Acoust., Speech, Sig. Process.*, vol. 25, no. 5, pp. 442–448, Oct 1977.

[47] D. H. M. Schellekens, T. Sherson, and R. Heusdens, "Quantisation effects in pdmm: A first study for synchronous distributed averaging," in *Proc. IEEE Int. Conf. Acoust., Speech, Sig. Process.*, March 2017, pp. 4237–4241.

[48] N. Shlezinger, Y. C. Eldar, and M. R. D. Rodrigues, "Hardware-limited task-based quantization," *IEEE Trans. Sig. Process.*, vol. 67, no. 20, pp. 5223–5238, 2019.

[49] P. Li, N. Shlezinger, H. Zhang, B. Wang, and Y. C. Eldar, "Task-based graph signal compression," *arXiv preprint arXiv:2110.12387*, Oct 2021.

[50] G. H. Golub and H. A. van der Vorst, "Eigenvalue computation in the 20th century," *J. Comput. Appl. Math.*, vol. 123, no. 1-2, pp. 35–65, Nov. 2000.

[51] S. M. Kay, *Fundamentals of Statistical Signal Processing: Estimation Theory*. Upper Saddle River, NJ, USA: Prentice-Hall, Inc., 1993.

[52] F. Gama, E. Isufi, A. Ribeiro, and G. Leus, "Controllability of bandlimited graph processes over random time varying graphs," *IEEE Transactions on Signal Processing*, vol. 67, no. 24, pp. 6440–6454, 2019.

[53] C. Hoppen, J. Monsalve, and V. Trevisan, "Spectral norm of oriented graphs," *Linear Algebra Appl.*, vol. 574, pp. 167–181, 2019.

[54] A. Ferrari and C. Richard, "Non-parametric community change-points detection in streaming graph signals," in *Proc. IEEE Int. Conf. Acoust., Speech, Sig. Process.*, 2020, pp. 5545–5549.

[55] A. Arguez, "Noaa's 1981-2020 u.s. climate normals: An overview," *Proc. Bull. Amer. Meteorol. Soc.*, pp. 1687–1697, 2012.

[56] P. Bodik, W. Hong, C. Guestrin, S. Madden, M. Paskin, and R. Thibaux, "Intel berkeley research lab data," 2004. [Online]. Available: http://db.csail.mit.edu/labdata/labdata.html

[57] S. K. Narang, A. Gadde, and A. Ortega, "Signal processing techniques for interpolation in graph structured data," in *Proc. IEEE Int. Conf. Acoust., Speech, Sig. Process.* IEEE, 2013, pp. 5445–5449.

[58] Y. Mao, G. Cheung, and Y. Ji, "Image interpolation for dibr viewsynthesis using graph fourier transform," in *3DTV-Conference: The True Vision-Capture, Transmission and Display of 3D Video (3DTV-CON), 2014*. IEEE, 2014, pp. 1–4.

[59] M. S. Mahmoud and M. Oyedeji, "Consensus in multi-agent systems over time-varying networks," *Cyber-Physical Systems*, vol. 6, no. 3, pp. 117–145, 2020.

[60] J. Saniuk and I. Rhodes, "A matrix inequality associated with bounds on solutions of algebraic riccati and lyapunov equations," *IEEE Trans. Autom. Control*, vol. 32, no. 8, pp. 739–740, Aug 1987.